Fractographic Inspection of the Cracking FT488/2 Removed at Program 79

S. Barter

DSTO-TN-0170

DEPARTMENT OF DEFENCE
DEFENCE SCIENCE AND TECHNOLOGY ORGANISATION

Fractographic Inspection of the Cracking in FT488/2 Removed at Program 79

S A Barter

Airframes and Engines Division
Aeronautical and Maritime Research Laboratory

DSTO-TN-0170

ABSTRACT

During the inspection of the FT488/2 Bare Bulkhead Fatigue Test specimen after 79 blocks of applied loading, cracking was found in several wing-attachment hole aft edges. Each of the cracked regions of the holes was cut from the bulkhead, sixteen of the cracks were broken open and the exposed crack surfaces were analysed. This analysis revealed several interesting aspects of fatigue crack growth in this bulkhead. These included the nature of the most (in this case) significant initiating flaws, the type (compared to other thick 7050 plate material) and effect of the microstructure on the growth of these cracks, and the relative growth rates of these cracks including estimates of the number of programs to failure.

DEPARTMENT OF DEFENCE

DEFENCE SCIENCE AND TECHNOLOGY ORGANISATION

Published by

DSTO Aeronautical and Maritime Research Laboratory
PO Box 4331
Melbourne Victoria
Telephone: (03) 9626 7000
Fax: (03) 9626 7089

AR-010-649
September 1998

Conditions of Release and Disposal

Fractographic Inspection of the Cracking FT488/2 Removed at Program 79

Executive Summary

During the inspection of the FT488/2 Bare Bulkhead Fatigue Test specimen after 79 blocks of applied loading, the starboard upper wing-attachment hole aft edge, port lower wing-attachment hole aft edge and the port upper wing-attachment hole aft edge, were found to have crack indications. This cracking was confirmed by dye penetrant inspection of the regions under load. Each of the cracked holes had multiple corner cracks, with crack depths estimated to be no more than 1 mm. With the bushes removed from the holes, the cracking appeared to be confined to the aft edges of the holes. To assess the true extent of the cracking, the crack growth rate and nature and influence of the initiating flaws, the areas containing the cracks were cut from the bulkhead. Sixteen of the cracks were broken open for analysis and several sections were cut adjacent to the cracked regions to assess the microstructure. Apart from the wing-attachment hole cracks, one of the four-inch radii (starboard forward) also had a crack indication. This area was removed. No cracking could be found although a defect in the ion vapour deposited aluminium coating in the region of the suspected crack was noted and was probably responsible for the indication.

The investigation of the wing-attachment hole cracking revealed some interesting aspects of fatigue in this material, and its interaction with flaws and the microstructure;

1. Cracking was very consistent in both the upper holes, while the lower hole cracking appeared to have been influenced by either a large flaw, with a large 'effective crack size', or a significant residual stress.
2. Cracks from the upper holes all started from flaws created by the IVD coating process - none were found to have initiated from inclusions.
3. For this material and spectrum, the crack growth seemed to be relatively unaffected by the microstructure once a crack had reached a size greater than about 10 μm.
4. The crack growth region can be depicted by a growth constant 'b' which allows extrapolation beyond the known data. This approach was also used to compare the severity of the different cracks, giving an indication of their expected life, and the effect of stressing, on the variation in crack growth rates from hole to hole.
5. The microstructure of the bulkhead in these regions was consistent with previously observed microstructure; this material still had structures indicative of minimal breakdown from the original ingot. The re-crystallised grains appear to have had an influence on relief of the crack surface near the origins of cracks - large grain structure therefore produced flat surfaces while fine grains produced rougher surfaces.

Contents

1. Introduction

During the inspection of the FT488/2 Bare Bulkhead Fatigue Test specimen after 79 blocks of applied loading, the starboard upper wing-attachment hole aft edge, starboard lower wing-attachment hole aft edge, and the port upper wing-attachment hole aft edge, were found to have crack indications. This cracking was confirmed by dye penetrant inspection of the regions under load. Each of the cracked holes had multiple corner cracks, with crack depths estimated to be no more than 1.5mm.

After removal of the bushes from the holes, the cracking appeared to be confined to the aft edges of the holes. To assess the true extent of the cracking, the crack growth rate and nature and influence of the initiating flaws, the areas containing the cracks were cut from the bulkhead for detailed examination.

One of the four-inch radii (starboard forward) also had a crack indication, so this region was also removed for examination.

The test had completed 79 programs, which equates to 25672 Simulated Flying Hours (SFH) using the IARPO3A spectrum. This spectrum was designed to represent CF and RAAF usage. In general, it differed from the USN spectrum (used in the first of the 488 Bulkhead fatigue tests carried out at AMRL [1]), by containing considerably more turning points (approx. 13k vs. 6k) and not as many high loads. Although the IARPO3A spectrum does not have as many high loads it does have a larger number of 5-7g loads and one 9g load which is higher than the highest load in the USN spectrum. Overall, the IARPO3A spectrum is considered more severe than the previous spectrum.

2. Examination

2.1 Area of cracking

The NDE examinations indicated cracking up to 1.5mm along the aft face of the bulkhead and 1mm down the bore of the wing-attachment holes. The positions of these cracks, as indicated in NDI report B38/97, are shown in Figures 1 & 2.

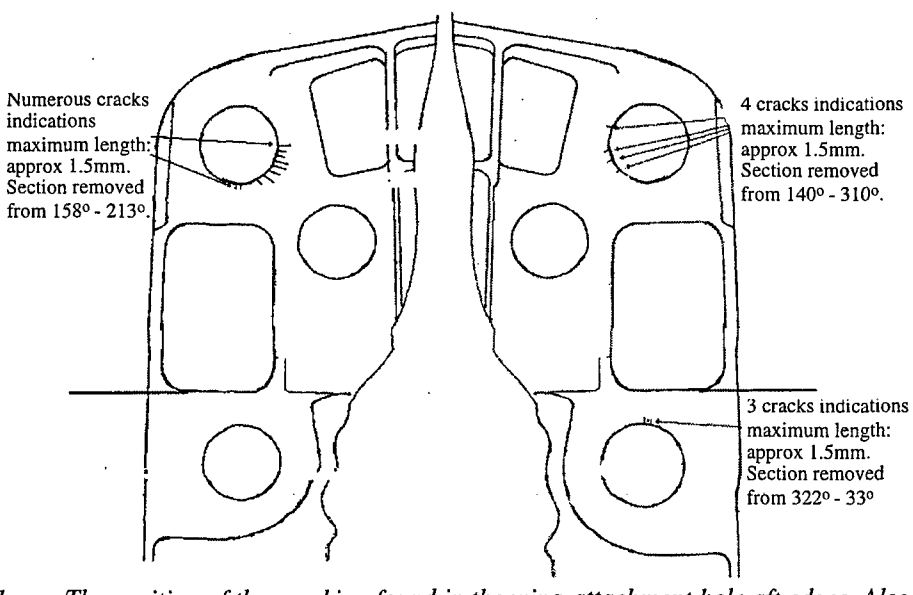

Figure 1. The position of the cracking found in the wing-attachment hole aft edges. Also, note the extent of the region removed is marked.

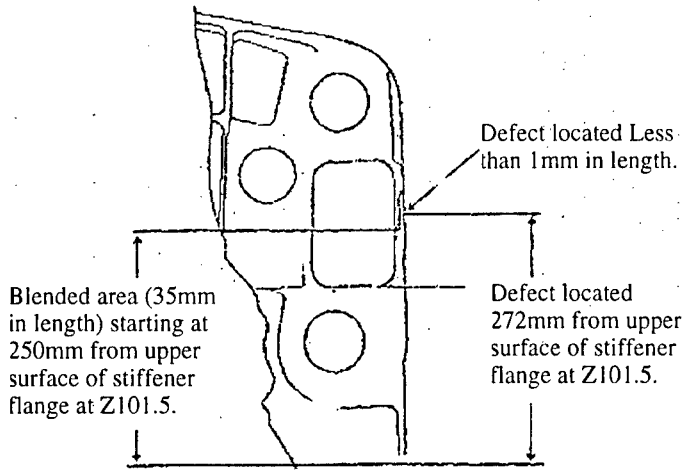

Figure 2 The position of the crack indication found in the 4" radius

Crescent shaped slivers of material were removed from each of the cracked holes using steel templates as guides, and a jeweller's hacksaw. The slivers were cut at 30° to the hole bores according to an agreed process. A crescent shaped section of the 4" radius, that had a crack indication, was also cut from the bulkhead. The areas from which material was excised are shown in Figures 3, 4, 5 and 6. The 4" radius area was polished to 600# finish after the removal of the region with the crack indication.

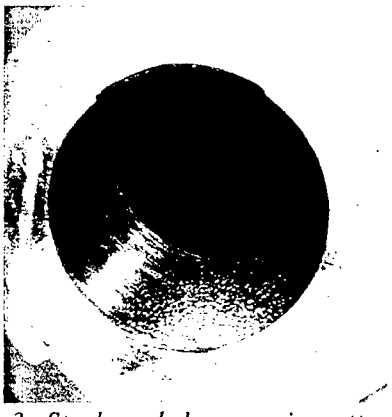

Figure 3 Starboard lower wing-attachment hole showing the cut in the upper part of the hole.

Figure 4 Starboard upper wing-attachment hole showing the cut in the port side and lower part of the hole

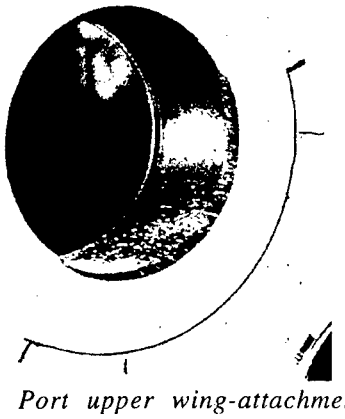

Figure 5 Port upper wing-attachment hole showing the cut in the starboard and lower side of the hole

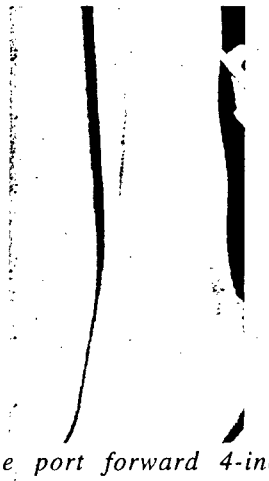

Figure 6 The port forward 4-inch radius showing the blended region that resulted from a previous removal of material and this removal. A blended region on the aft face is also visible.

2.2 Examination sections removed

The sliver removed from the port forward 4"radius was inspected and loaded in three point bending to reveal any cracks present. No cracking was observed, rather, a defect in the IVD coating at about the position of the suspected crack was found and probably accounts for the NDI indication.

All of the sections removed from the wing-attachment holes aft edges were found to contain cracks. An example is shown in Figure 2A, which has been partially opened (note that the jagged part of this crack is the result of the opening). On stressing the starboard upper section revealed 7 crack locations, the starboard lower section 3 crack locations and the port upper section 11 crack locations. Several of these crack locations had two closely associated cracks, as shown in Figure 2B. Schematic diagrams of the approximate positions of the observed cracks and the material removed, are shown in Figure 3.

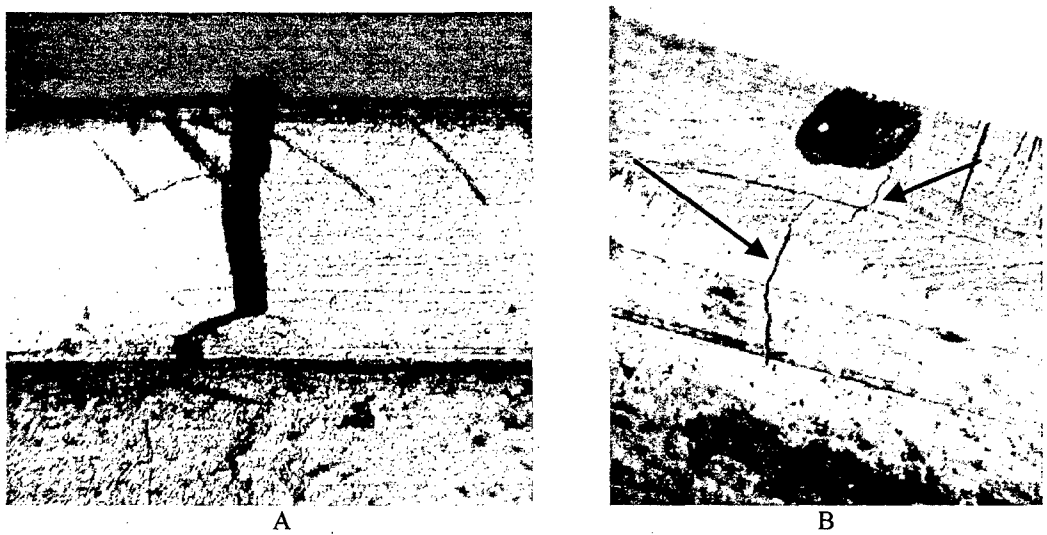

Figure 2. Examples of two of the cracks revealed in the section removed from the port wing-attachment hole upper aft edge. Both of these views were taken with the cracking loaded. View 'A' shows a ridge on the hole surface – the fatigue part of the crack is the vertical part, that which follows is tearing due to the applied opening load. In 'B' the corner is roughly in the middle of the field with the hole-surface on the lower side and the aft face of the bulkhead on the upper side. Note that two cracks exist in this location, the second independent of the hole surface or edge.

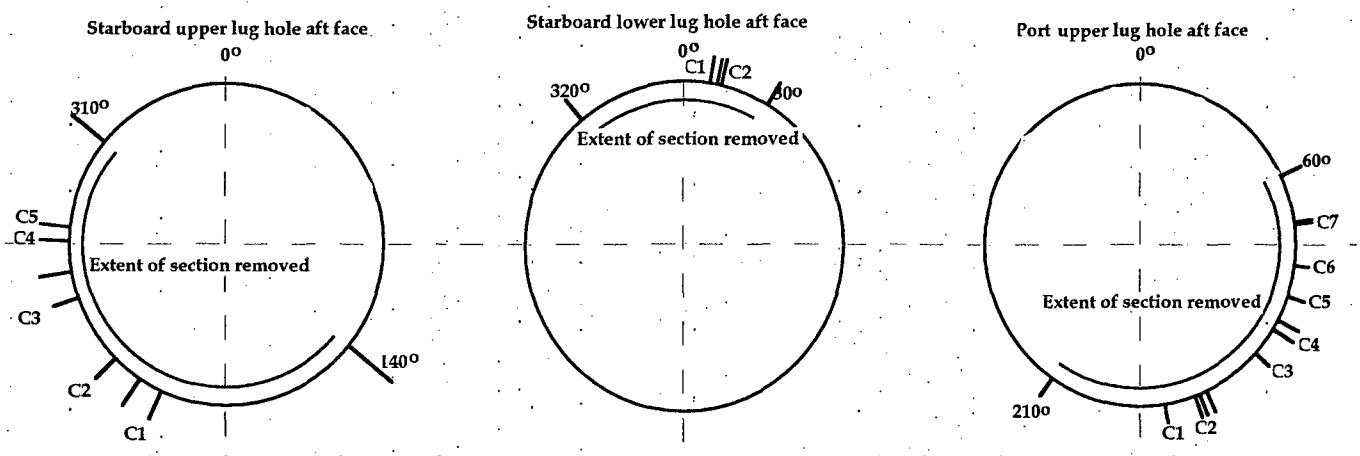

Figure 3. A schematic diagram of the approximate positions of the observed cracks in the edge of the wing-attachment holes. The red line indicates the region of material removal. The cracks that were opened and examined by fractography are marked 'C1, C2, etc'.

During the examination of the removed sections, and the cracks that were contained in them, it was noticed that in all three pieces removed from the wing-attachment holes a ridge existed close to the edge, on the hole surface. This ridge, in each case, was a short distance from the outer edge of the holes. (An example of this ridge is shown in Figure 2A). In all cases, the cracking was confined to the region between the edge of the hole and the ridge. This ridge appears to have been caused by the edge of the copper alloy bushes, which were fitted to these holes, not extending to the outer edge. This meant that when the copper alloy bushes were cold-expanded their edge formed a ridge in the hole surface.

2.3 Examinations of individual cracks

Several of the cracks observed in each of the slivers were broken open, first examined in the SEM, and then examined by quantitative fractography. A distinct repeating pattern could be observed in several areas of most cracks and a less distinct pattern could be observed in other regions of these cracks. The combination of these regions allowed a relatively complete picture of the crack growth to be assembled for each of the cracks opened. To complete this task, some assumptions were made: each repeat of the pattern is equivalent to a single load block or program. This assumption is supported by previous examinations of bulkhead material, which have undergone similar fatigue testing. These tests produced repeating markings that were found consistent with the type and spacing expected for fatigue growth per program under these conditions.

The method of calculating the crack depth during measurement of the crack growth curves is to take an 'x' and 'y' reading from a zero position set at the surface below the initiation, rather than measuring the distance tracked during the measuring process. The 'x' and 'y' positions are fitted to a circular model ie. the depth of a particular mark is the calculated radius to the position of the mark from the initiation point. This procedure is carried out since it is hardly ever possible to track the growth along a straight line from the initiation to the deepest point of the crack. Since most fatigue cracks are not semi-circular in shape, the further that the measurements wander from the line between the origin and the deepest reading, the more error may be incorporated into the results. Nevertheless, if care is taken to keep close to the line between the origin and the deepest point (or reading) of the crack, the resulting crack growth curve will usually provide a good representation of the crack growth rate.

The final difficulty with tracking the growth of fatigue cracks in aluminium alloy 7050 is the tendency for the repeating pattern to change considerably during the crack growth. This occurs due to the increasing effect of lower loads as the crack progress. While during early crack growth the highest loads in the 'program' may distinguish the pattern and therefore the repeat may appear to be very distinct, as the crack becomes deeper the loads that are nearly as high will start to produce markings similar to the high loads, changing the patten. This patten will continue to change as the loads increase, and the markings made by the peak loads change in character. This results in a very confusing set of marks on the crack surface, in the latter stages of the crack growth. The 'program' repeats may again become clear near the end of crack growth, since the peak load will usually be the first to produce tear bands on the fracture surface. Fortunately, in this case all the cracks were of a small size with relatively distinct programs being discernible even near the ends of the crack.

Notwithstanding the limitations and assumptions outlined above, several crack measurement sequences representing the positions of the 'program' repeats were

determined to produce the crack growth results presented in the following sections. The crack path taken in each case did not necessarily result in a crack depth that was equal to the deepest point of the crack. The growth curves are presented along with images of each of the cracks. The areas that gave the greatest difficulty for quantitative fractography were those that were very close to the origin and, therefore these regions of the crack growth curves may have the least confidence.

2.3.1 Crack dimensions

As each crack was opened the dimensions set out in Table 1 were taken. These figures refer to the dimensions marked in the schematics Figure 4.

Table 1 Dimensions of the cracks broken open and examined (see Figure 4)

Crack ID	Dimension A	Dimension B	Dimension C
STBD upper crack 1	0.36mm	1.02 mm	0.19 mm
STBD upper crack 2	0.54 mm	1.35* mm	-
STBD upper crack 3	0.64 mm	1.43 mm	-
STBD upper crack 4	0.44 mm	1.19 mm	-
STBD upper crack 5	0.62 mm	0.79 mm	-
STBD Lwr crack 1	0.74 mm	0.70 mm	-
STBD Lwr crack 2	0.82 mm	0.93 mm	-
Port upper crack 1	0.88 mm	1.27 mm	-
Port upper crack 2	0.59 mm	1.43* mm	-
Port upper crack 3	0.79 mm	1.32 mm	-
Port upper crack 4	0.70 mm	1.11 mm	-
Port upper crack 5	0.75 mm	1.26 mm	-
Port upper crack 6	0.52 mm	1.18 mm	-
Port upper crack 7	0.59 mm	1.11 mm	-

* Not all of crack was captured in the piece removed

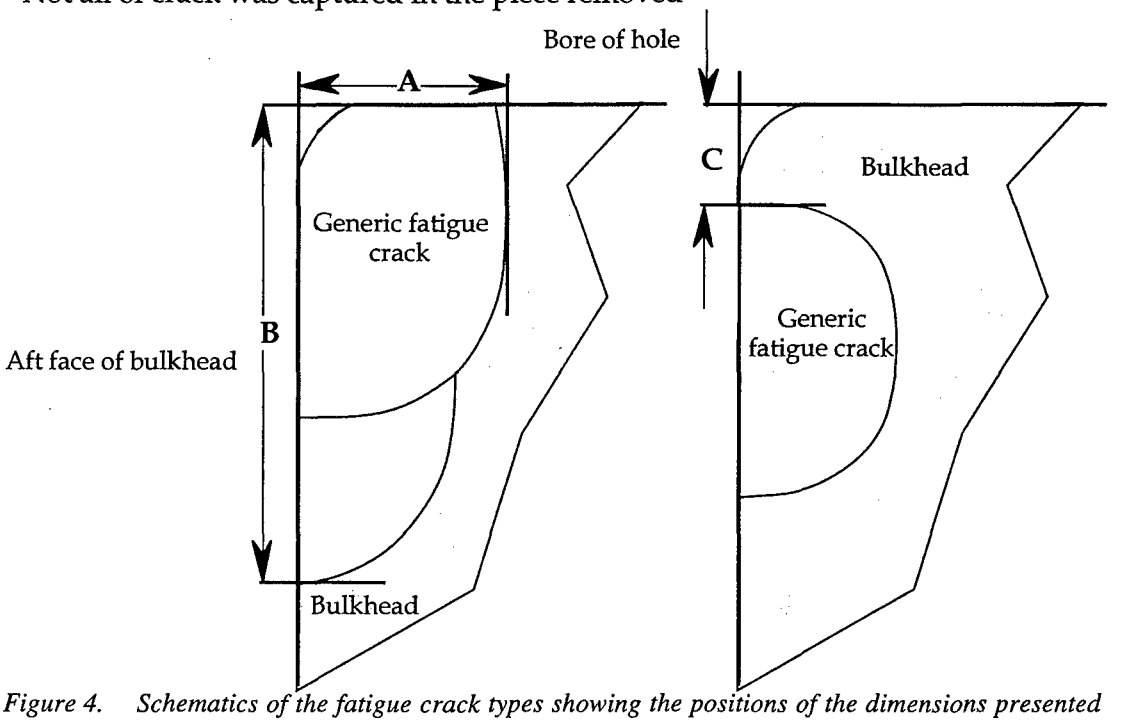

Figure 4. Schematics of the fatigue crack types showing the positions of the dimensions presented in Table 1

2.3.2 Starboard upper aft edge - Crack 1

This crack originated some distance from the wing-attachment hole and, growing with a 'thumbnail' shape, remained independent of the hole surface for its entire life. The actual originating flaw had been removed by polishing during the test. The crack is shown in Figure 5 view A and a close up of the region from which the fractography measurements were started is shown in view B. This region is displaced somewhat from the region that would have been closest to the origin, being chosen for the most viewable markings.

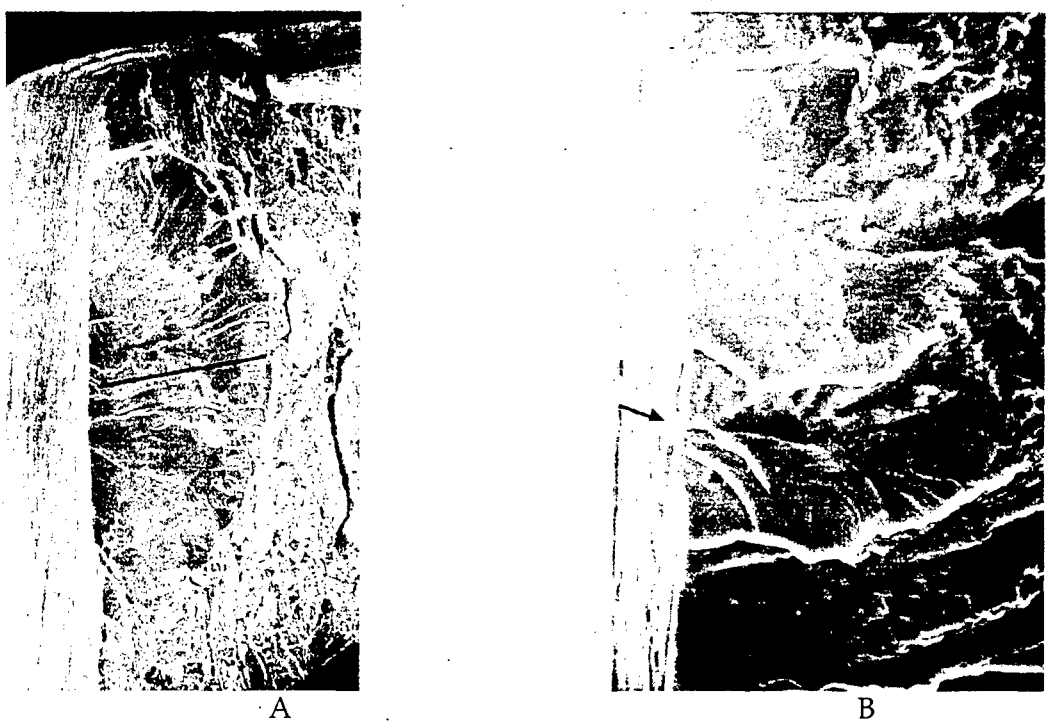

Figure 5. This Figure shows the crack profile and initiation region. The line shown in view A designates the approximate line followed during fractography. The origin has been polished off during the testing. The area from which the fractographic readings were initiated is marked with an arrow in view B.

Figure 6 shows the quantitative fractographic examination results for this crack.

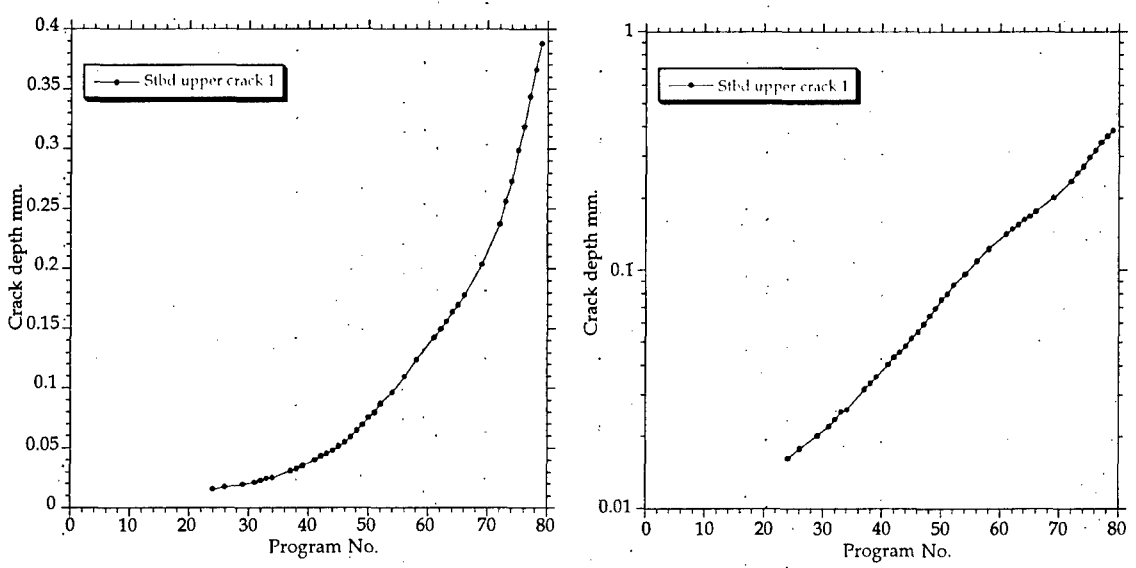

Figure 6. Two plots showing the results of quantitative fractography. Plot A – linear crack depth versus Program No. and B - crack depth on a Log scale versus linear Program No.

2.3.3 Starboard upper aft edge - Crack 2

This crack originated from multiple sites beneath the intact IVD (Ion Vapour Deposited aluminium) coating on the aft face of the bulkhead, Figure 7. The IVD appears as a dark layer of columnar grains at the left of view B Figure 7. Two main areas of initiation resulted in two similarly sized cracks, view A Figure 7. It appears that small grain boundary penetrations, probably caused by etching during the application of the IVD coating, acted as the initiating flaws, Figure 7 view B. The cracks grew as a series of 'thumbnail' shaped cracks, which linked to form a broad crack front for both major cracks. These cracks were growing forward into the bulkhead. Intersection with the wing-attachment hole probably occurred when the crack had reached a depth of about 100μm. At that time the crack closest to the hole was probably independent of the second crack, which had initiated further from the hole

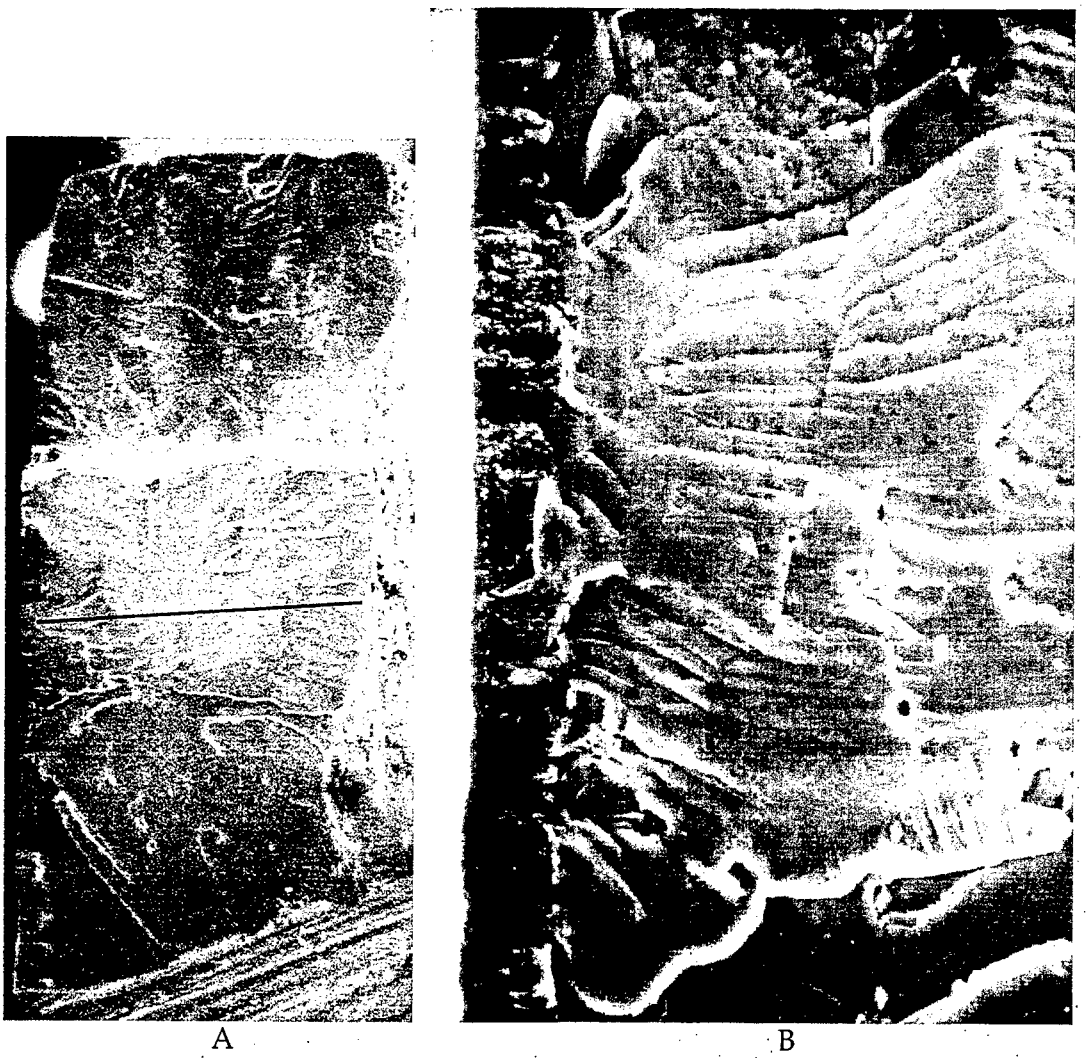

A B

Figure 7. Views of the profile of crack 2 and the initiation area. The line shown in view A designates the approximate line followed during fractography. The cracking initiated beneath the IVD on the aft surface of the bulkhead. The cracking originated at surface etching rather than any other more pronounced flaw

Quantitative fractographic examination of the second crack gave the results as set out in Figure 8.

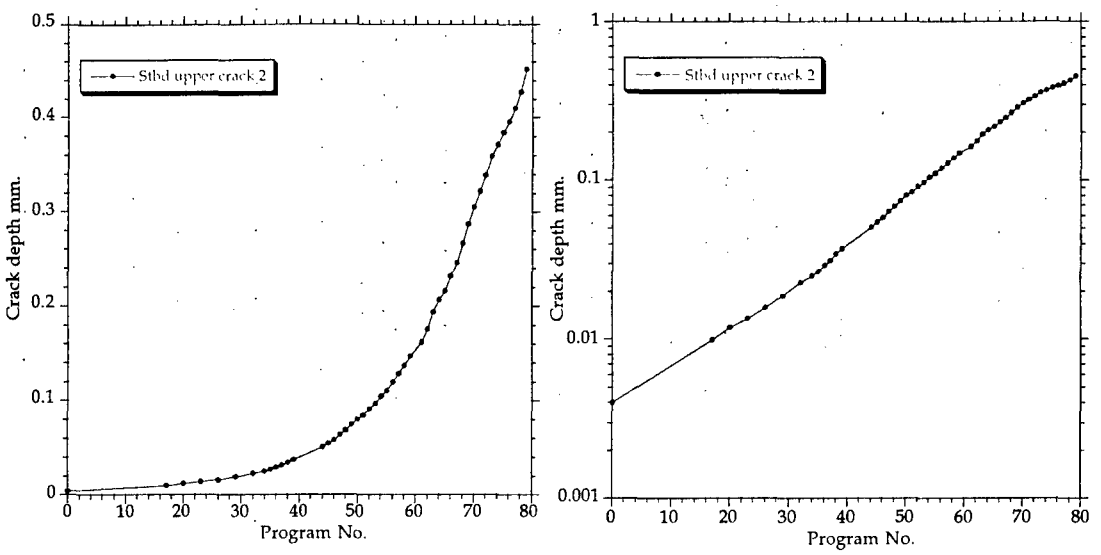

Figure 8. Two plots showing the results of quantitative fractography. Plot A – linear crack depth versus Program No. and B - crack depth on a Log scale versus linear Program No

2.3.4 Starboard upper aft edge - Crack 3

This crack originated from multiple sites beneath the intact IVD on the bulkhead aft face. Two cracks grew from two main areas of initiation. These cracks joined to form a single crack front, Figure 9A. Small etch-pits, probably associated with grain boundaries as in crack 2, acted as the initiating flaws. Both the main crack initiations appear to have grown along a grain boundary during their very early growth, Figure 9B and C. The cracks grew forward into the bulkhead as a series of thumbnail shaped cracks, which linked to form a broad crack front. Wing-attachment-hole intersection probably occurred at a crack depth of about 150µm, for the crack closest to the hole. At this time, this crack was probably independent of the second major crack, which had initiated further from the hole.

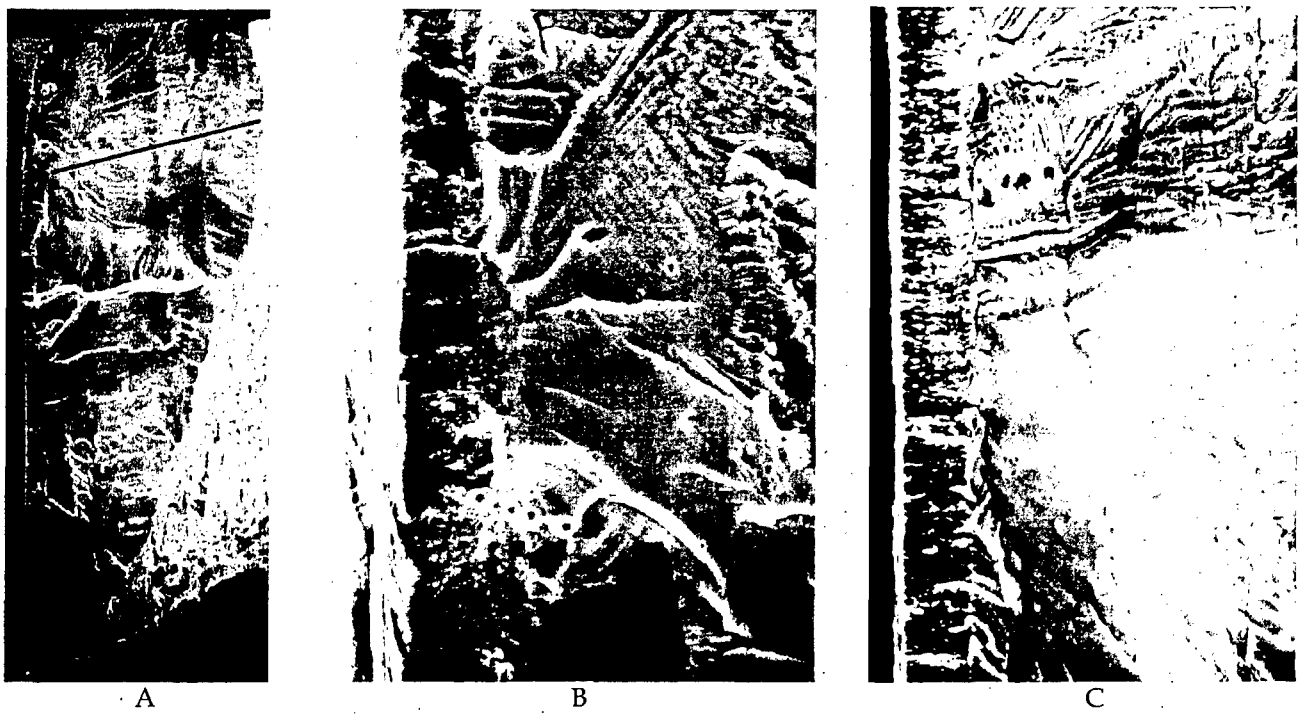

A B C

Figure 9. The crack profile and initiation areas of the two major cracks. View A has a line that indicates the approximate path followed during fractography. The cracking initiated beneath the IVD at the surface of the 7050. The two major origins are shown (fractography was carried out on the origin in view B).

Quantitative fractographic examination of the crack marked in the above Figure, initiating from the origin shown in view B gave the results as set out in Figure 10.

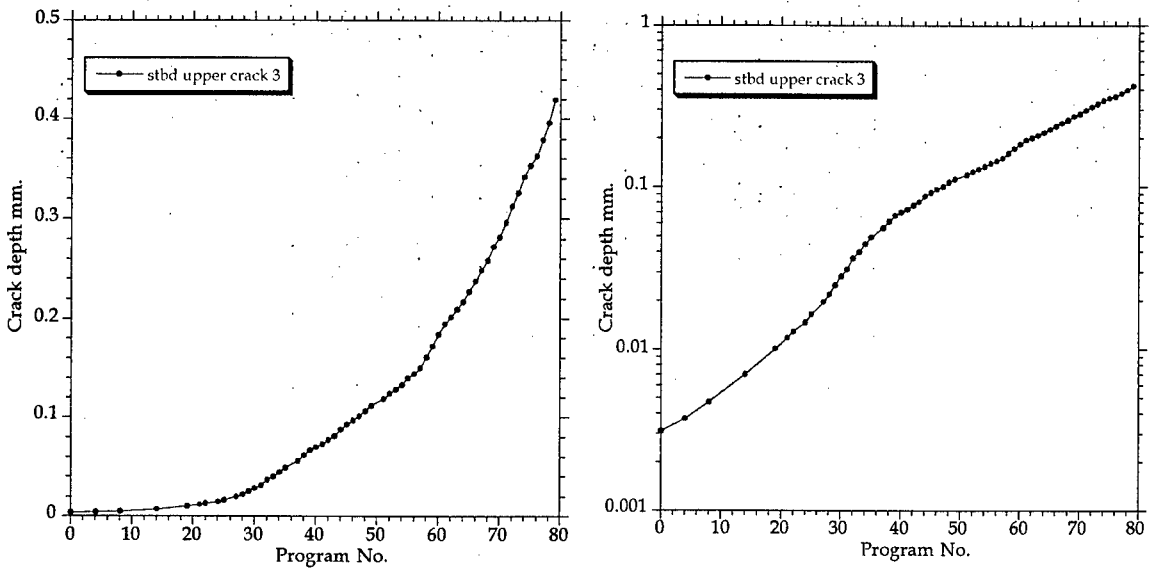

Figure 10. Two plots showing the results of quantitative fractography. Plot A – linear crack depth versus Program No. and B - crack depth on a Log scale versus linear Program No.

2.3.5 Starboard upper aft edge - Crack 4

In this case, the main crack origin occurred some distance from the wing-attachment-hole. The crack grew with a 'thumbnail' shape and remained independent of the wing-attachment hole for a large part of its life. The actual originating flaw had been removed by polishing during the test. The crack is shown in Figure 11A, while view B shows a close up of the region from which the fractography measurements were started.

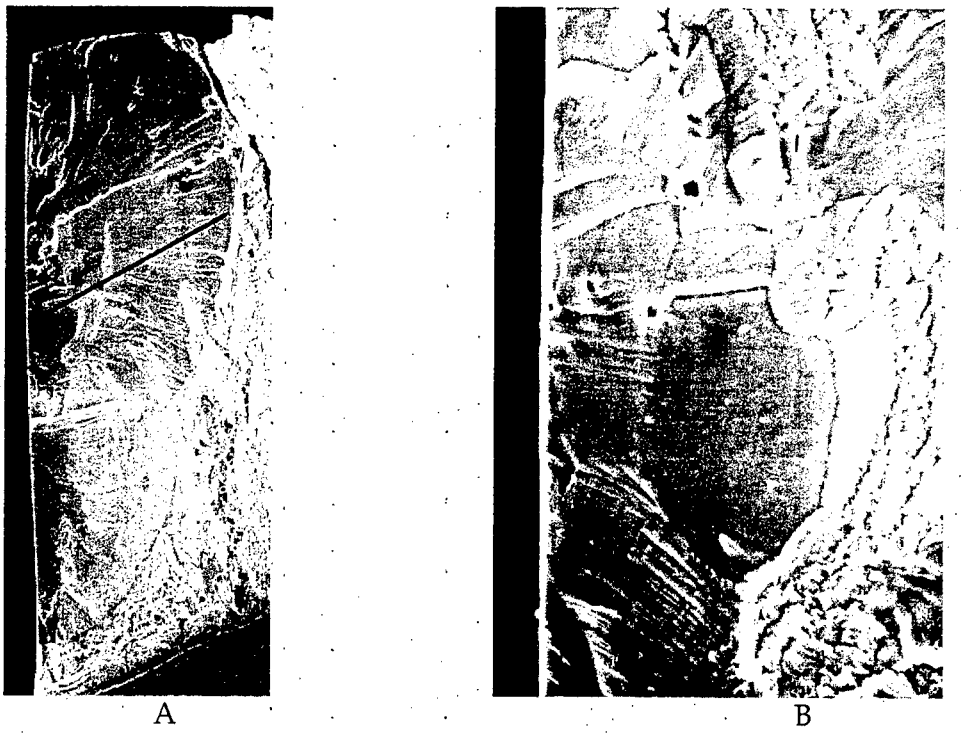

Figure 11. Views of the crack profile and initiation area, showing, in view A, the approximate line followed during fractography.

Quantitative fractographic examination of this crack gave the results as set out in Figure 12.

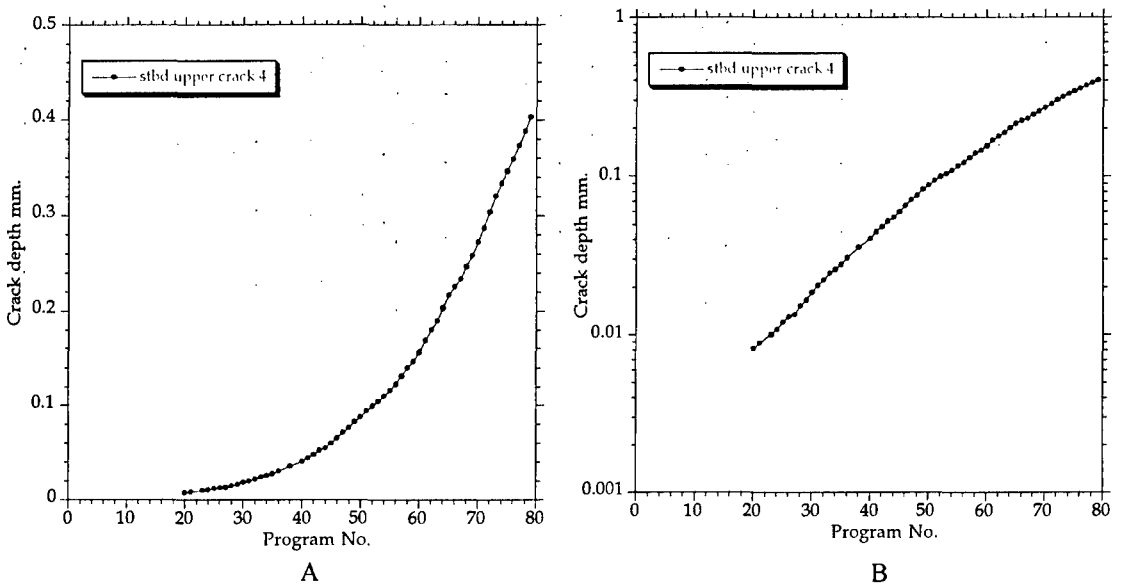

Figure 12. Two plots showing the results of quantitative fractography. Plot A – linear crack depth versus Program No. and B - crack depth on a Log scale versus linear Program No.

2.3.6 Starboard upper aft edge - Crack 5

This crack, originated from multiple sites beneath the intact IVD coating on the aft face of the bulkhead, Figure 13A. Again small etch-pits, probably associated with grain boundaries, acted as the initiating flaws, with the initial crack growing along a grain boundary, Figure 13B. Intersection with the wing-attachment hole probably occurred at a crack depth of about 50μm.

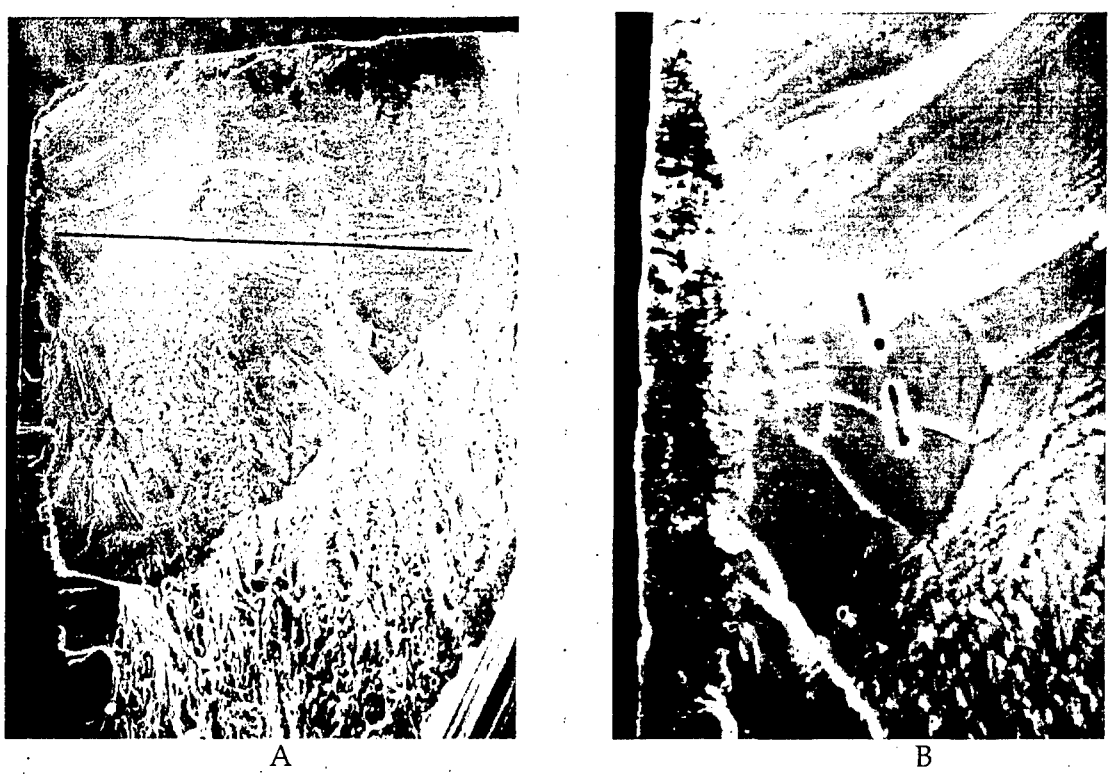

Figure 13. 'A' shows the crack profile and the line indicating the approximate path followed during fractography. View B shows the initiation site. Note some porosity in the middle of view B, which had no apparent effect on the crack growth.

Figure 14 shows the quantitative fractographic examination results for this crack.

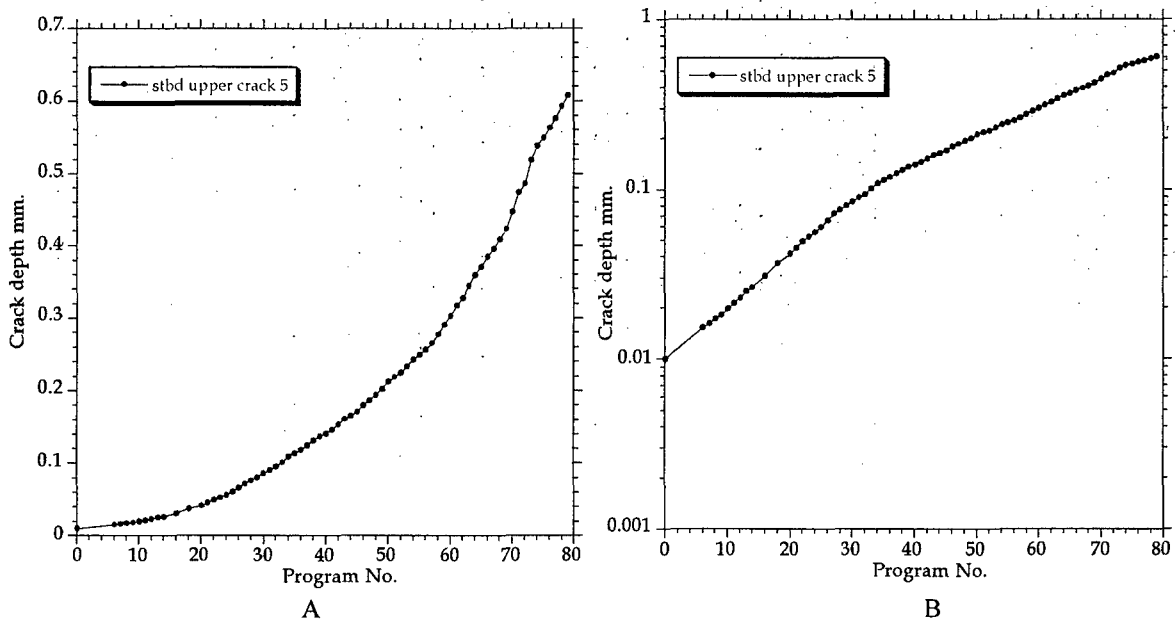

Figure 14. Two plots showing the results of quantitative fractography on crack 5. Plot A – linear crack depth versus Program No. and B - crack depth on a Log scale versus linear Program No.

2.3.7 Starboard lower aft edge - Crack 1

This crack initiated from a lip formed though mechanical damage to the edge of the hole. The crack appeared to have grown very quickly through the lip before commencing slow growth in to the bulk of the bulkhead. No microstructural detail could be discerned as aiding in the initiation of this crack. For the majority of its life, the crack grew as a corner crack. Figure 15A shows the entire crack and 15B a close up of the lip. Figure 16 shows the crack and the damage to the edge of the hole. It can be seen that the damage was caused by something producing a groove in the edge of the hole, possibly the wing- attachment pin or the alignment device. Figure 16 also shows the step in the bore of the hole, which was made by the copper alloy bush during cold expansion.

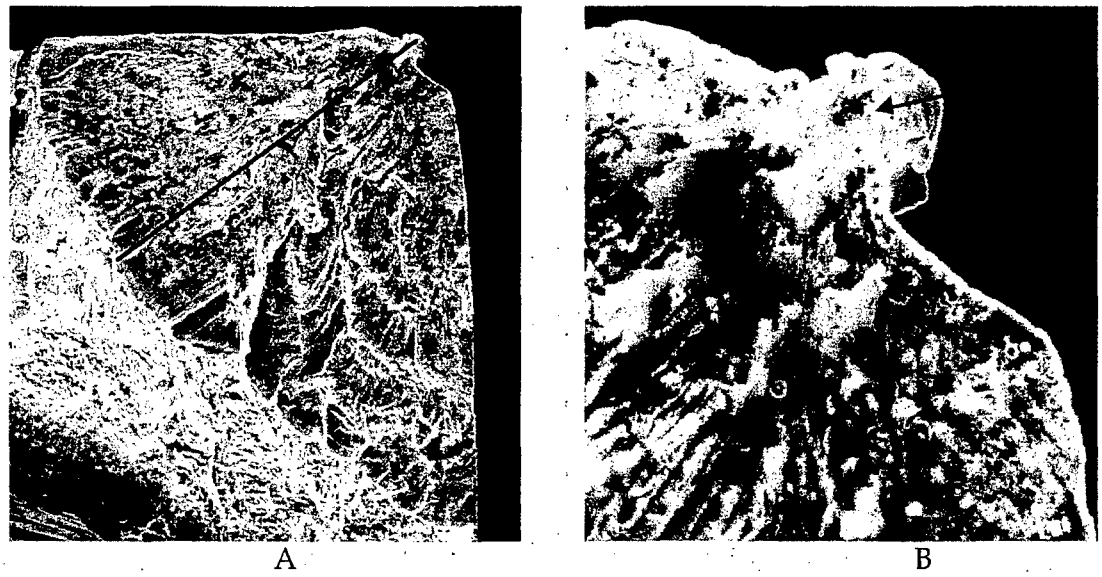

Figure 15. The crack profile and the initiation area of crack 1. Note that the initiation is associated with a lip caused by damage to the edge of the hole. The line shown in view A designates the approximate line followed during fractography. Cracking initiated in the lip (arrow).

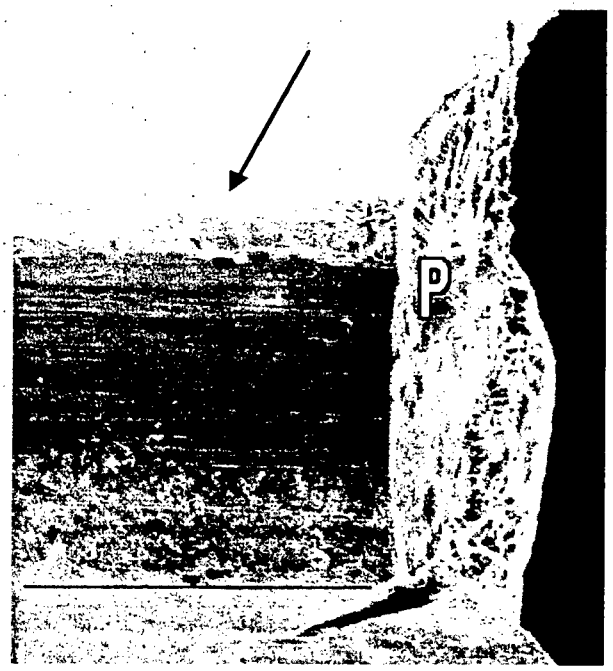

Figure 16. The crack as viewed from the bore of the hole, showing the crack P, the groove (arrow) and the position of a step in the hole bore surface that corresponded to the edge of the bush (line).

Quantitative fractographic examination gave the results as set out in Figure 17. The nature of the lip precluded estimating the flaw size, although an examination of the growth as depicted by the fractography indicates that the 'effective initial crack' size was about 45μm. Although it is possible that the damage, and therefore the crack initiation, occurred some time after the start of the test, the fractography suggest that it occurred very early, if not at the start of the test. Some residual stress effect may have been present as evidenced by the slight change in the slope of 'B' in Figure 17, although this effect must have been small.

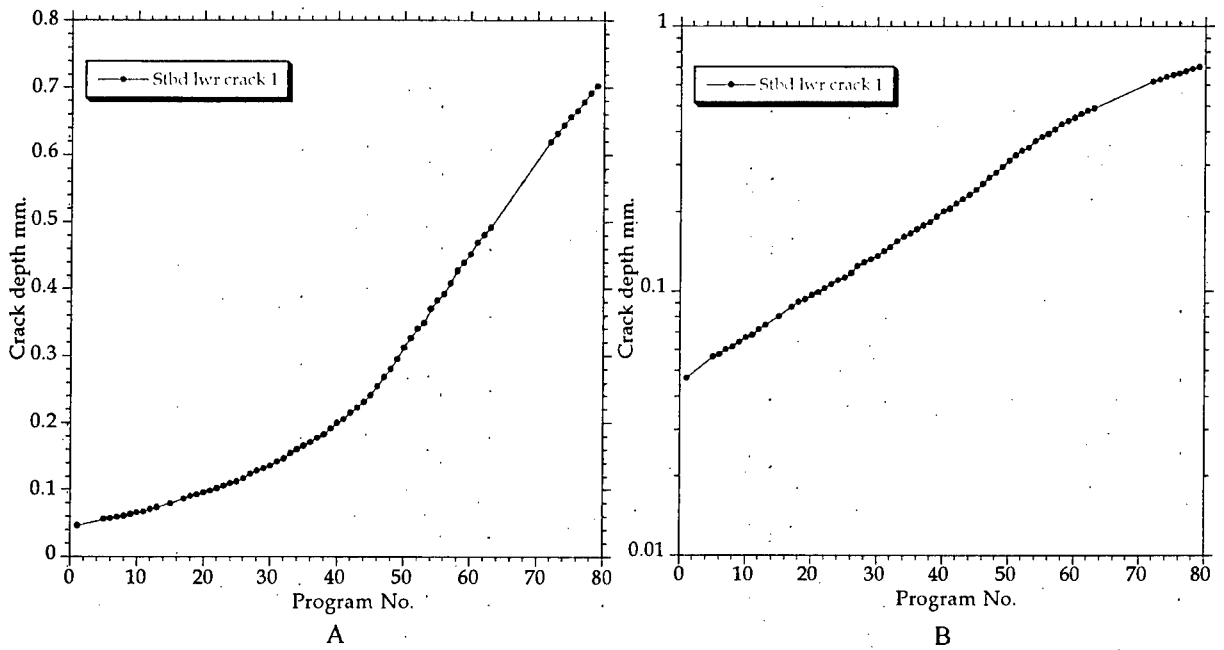

Figure 17. Two plots showing the results of quantitative fractography on crack 1. Plot A – linear crack depth versus Program No. and B - crack depth on a Log scale versus linear Program No.

2.3.8 Starboard lower aft edge - Crack 2

This crack also initiated from the starboard lower wing-attachment hole at the back of a lip formed by damage to the edge of the hole. Again, no microstructural detail could be seen to have affected the initiation of this crack. The crack grew for the majority of its life as a corner crack. The entire crack is shown in Figure 18A, a close up of the initiation region is shown in 'B'.

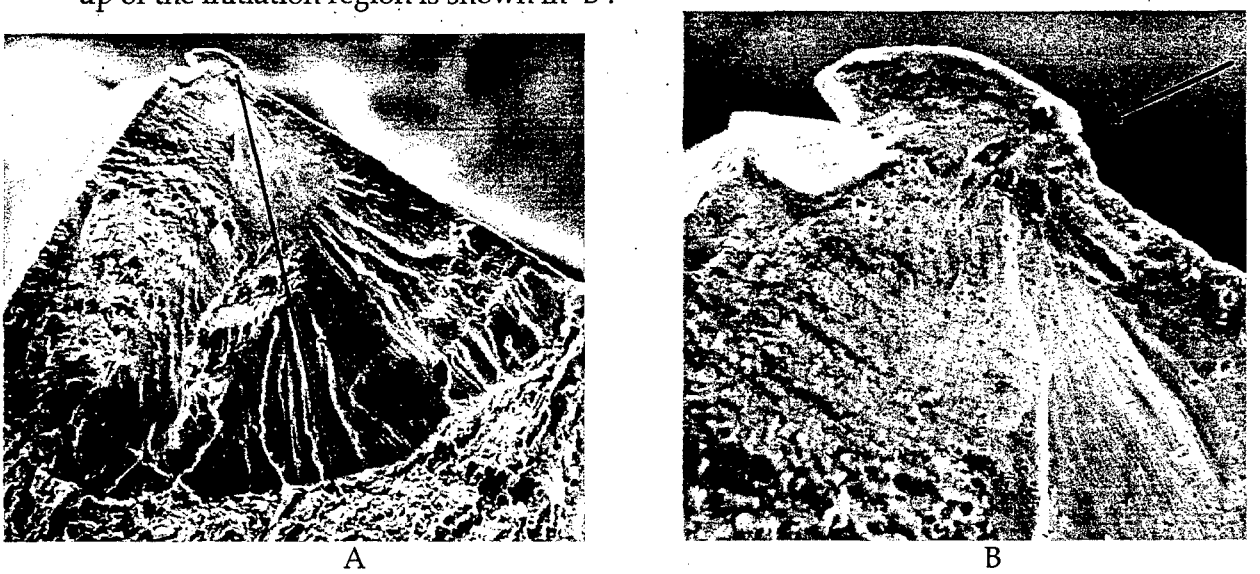

Figure 18. The crack profile and initiation area of the second crack in the starboard lower aft wing-attachment wing-attachment-hole edge. Note that the initiation is associated with a lip caused by damage to the edge of the hole. The line shown in view A designates the approximate line followed during fractography. Cracking initiated on the hole bore surface at the back of the lip (arrow).

Figure 19 shows the quantitative fractographic examination results for this crack.

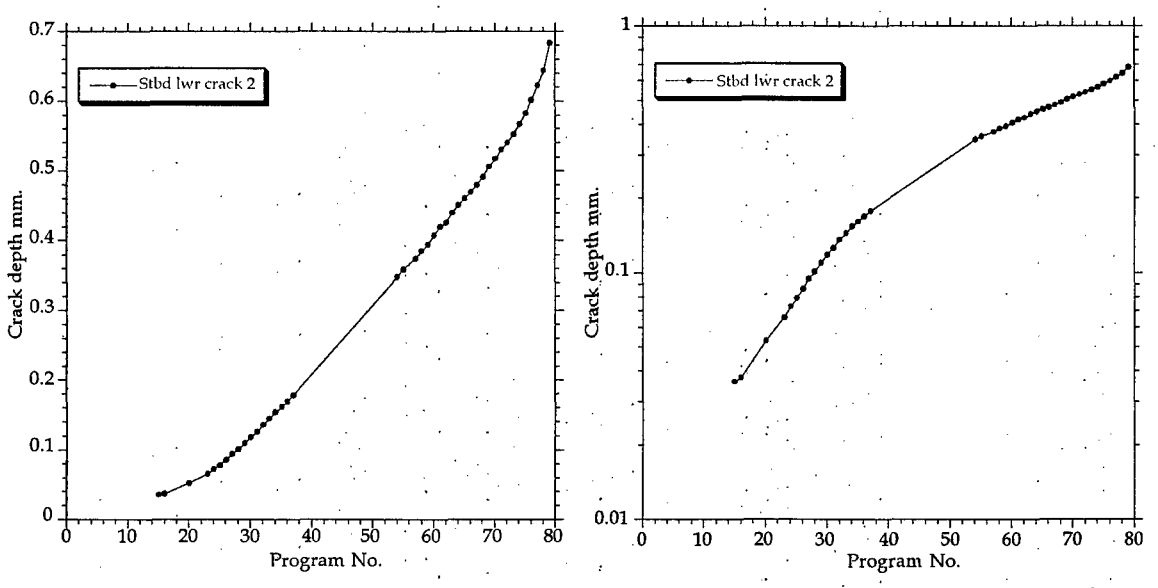

Figure 19. Two plots showing the results of quantitative fractography. Plot A – linear crack depth versus Program No. and B - crack depth on a Log scale versus linear Program No.

2.3.9 Port upper aft edge - Crack 1

This crack initiated from beneath the IVD coating on the aft face of the bulkhead. It appears that a small etch pit, probably associated with a grain boundary, initiated the cracking. The crack grew as an edge crack becoming a corner crack later in its life.

The entire crack is shown in Figure 20A and a close up of the initiation region is shown in 'B'.

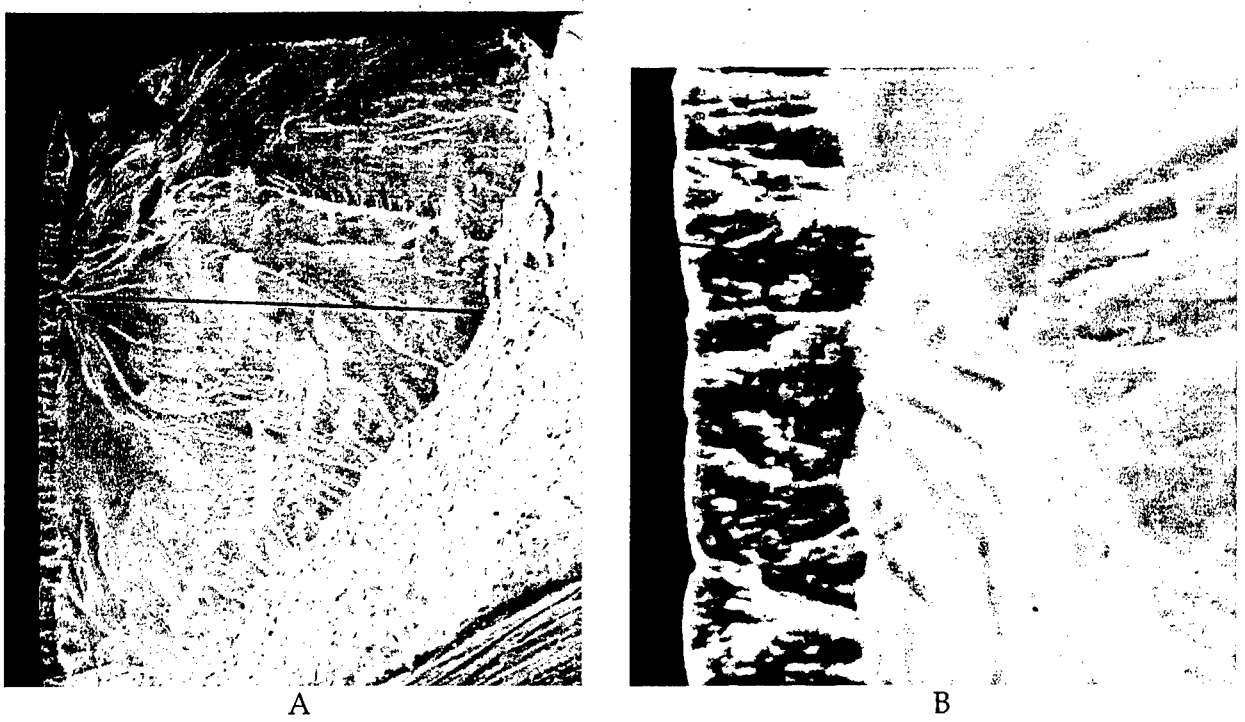

Figure 20. This Figure shows the crack profile and the initiation area of this crack. The line shown in view A designates the approximate line followed during fractography. Cracking initiated beneath the IVD at the surface of the 7050, view B.

Quantitative fractographic examination of this crack gave the results shown in Figure 21.

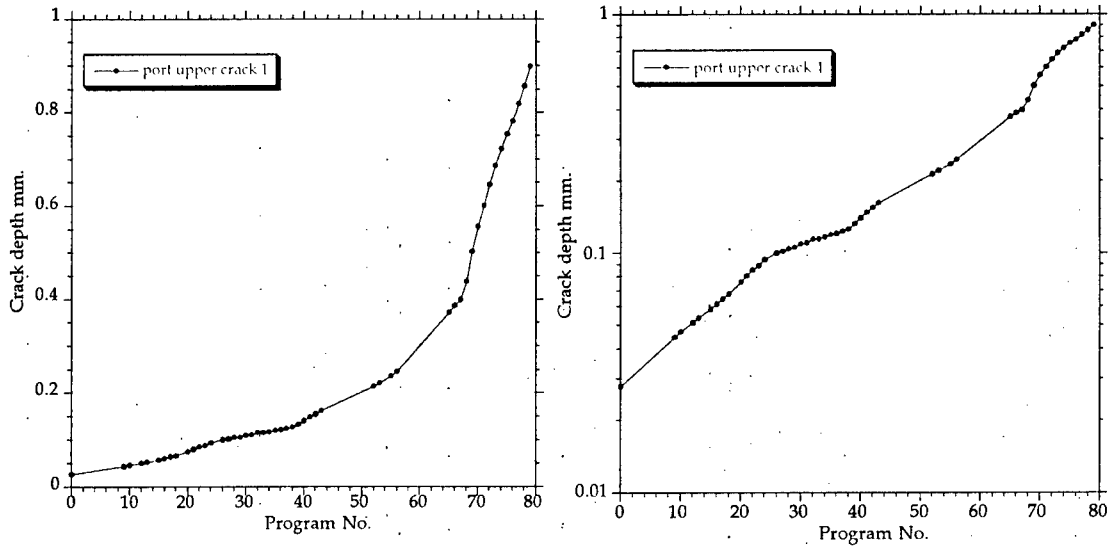

Figure 21. Two plots showing the results of quantitative fractography. Plot A – linear crack depth versus Program No. and B - crack depth on a Log scale versus linear Program No.

2.3.10 Port upper aft edge - Crack 2

This crack originated from multiple sites beneath the intact IVD coating on the aft face of the bulkhead. These sites were spread over about a 0.5mm length centred about 0.5mm from the hole edge. The numerous cracks joined to form a single crack front, Figure 21A. Small etch-pits, probably associated with grain boundaries, acted as the initiating flaws. Intersection with the wing-attachment hole probably occurred relatively late in the crack growth life - at a crack depth of about 200µm.

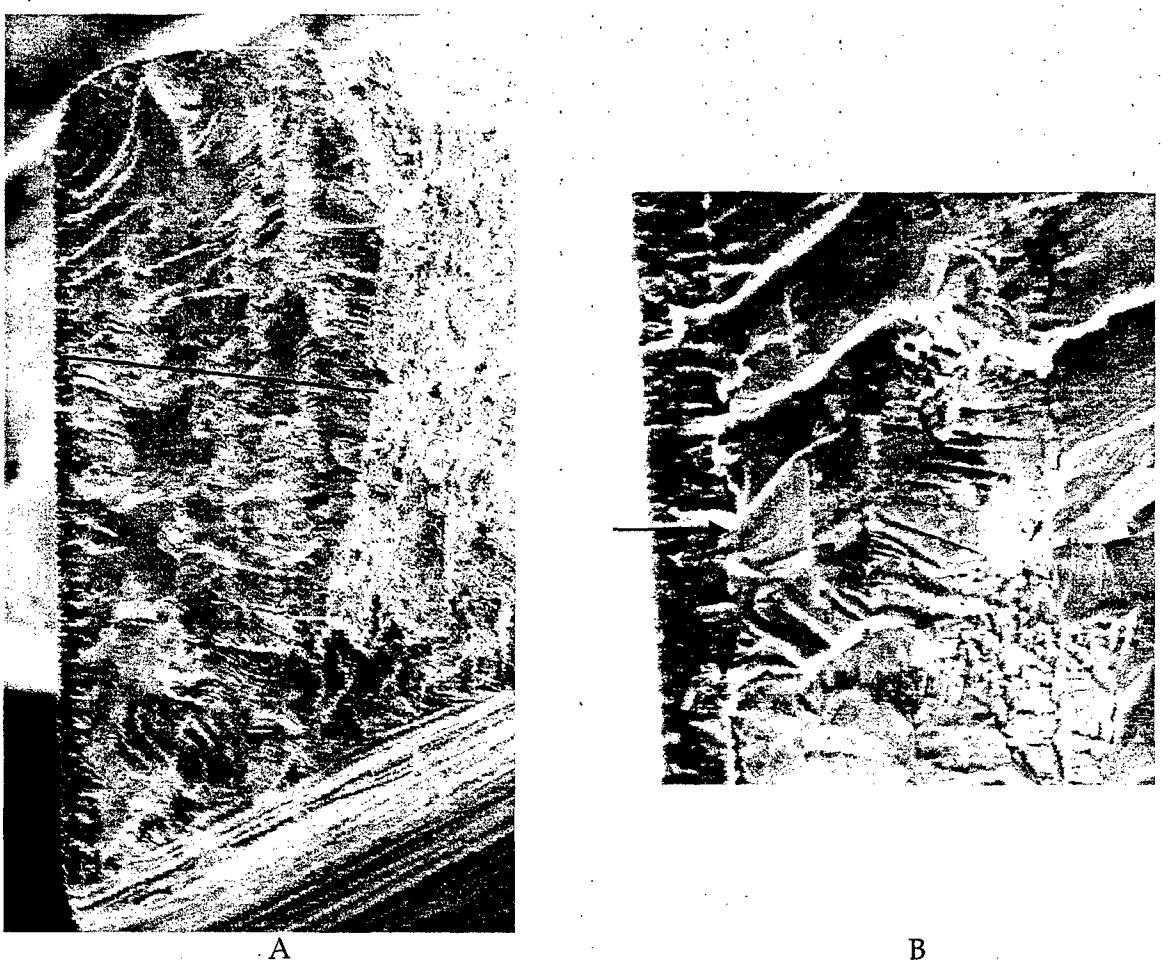

A B

Figure 21. The line shown in view A designates the approximate line followed during fractography. The cracking initiated beneath the IVD at the surface of the 7050. The initiation site used in the fractography is marked with an arrow.

Quantitative fractographic examination of this crack gave the results as set out in Figure 22.

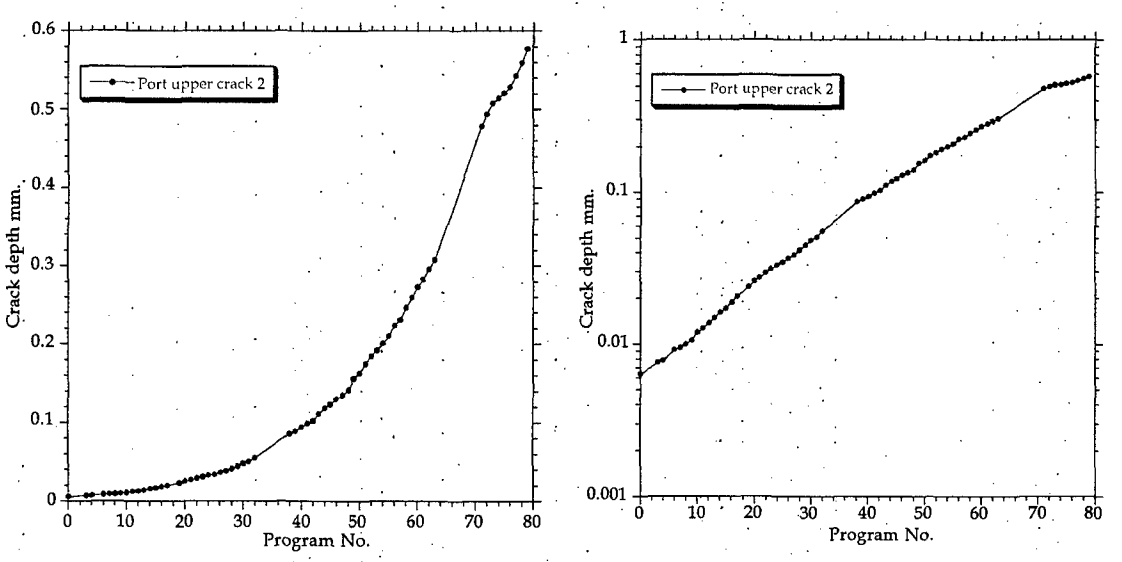

A B

Figure 22. Two plots showing the results of quantitative fractography. Plot A – linear crack depth versus Program No. and B - crack depth on a Log scale versus linear Program No.

2.3.11 Port upper aft edge - Crack 3

This crack originated from multiple origins beneath the IVD coating on the aft face of the bulkhead. The origins were closely spaced, centred at a distance of about 750μm from the hole edge, Figure 23A. Small etch-pits, probably associated with grain boundaries, acted as the initiating flaws. The crack's main initiation appears to have been associated with a grain boundary - the crack followed this boundary during its very early growth, view B. Intersection with the wing-attachment-hole occurred late in the crack growth life - at a crack depth of about 300μm.

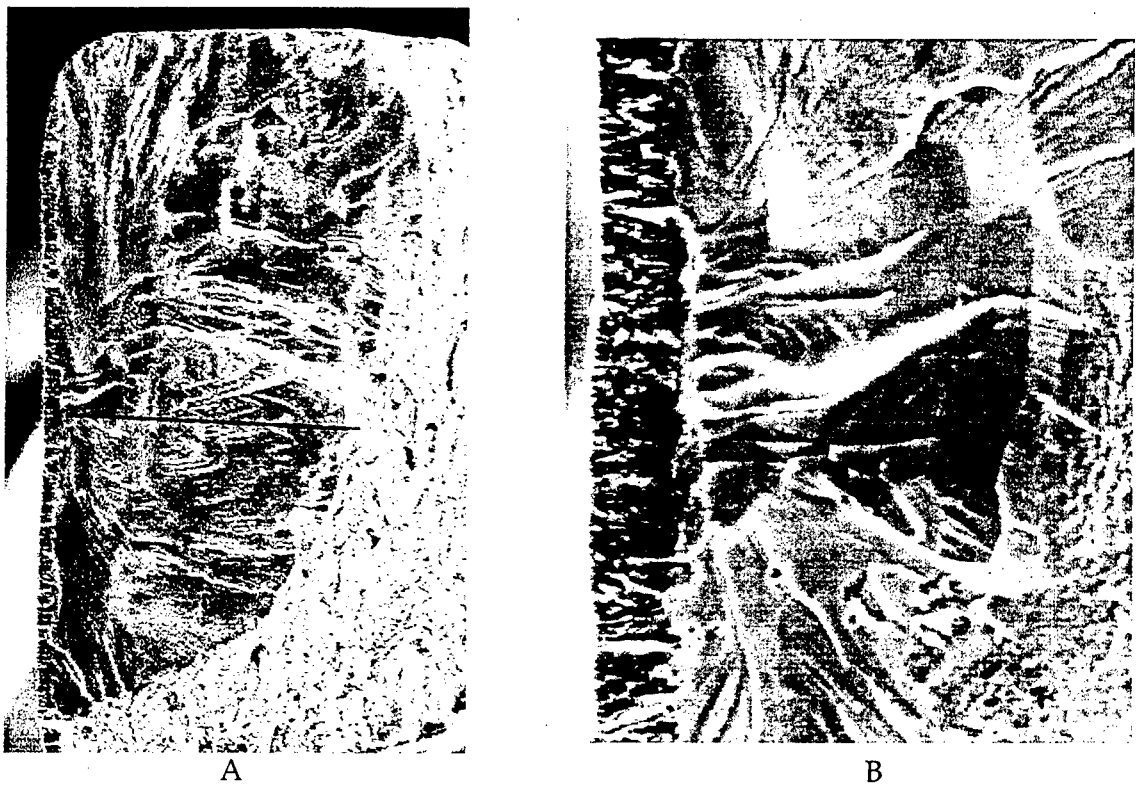

A B

Figure 23. This Figure shows the profile of crack 3 and its initiation area. The line shown in view A designates the approximate line followed during fractography. The cracking initiated beneath the IVD at the surface of the 7050.

Quantitative fractographic results for this crack are set out in Figure 24.

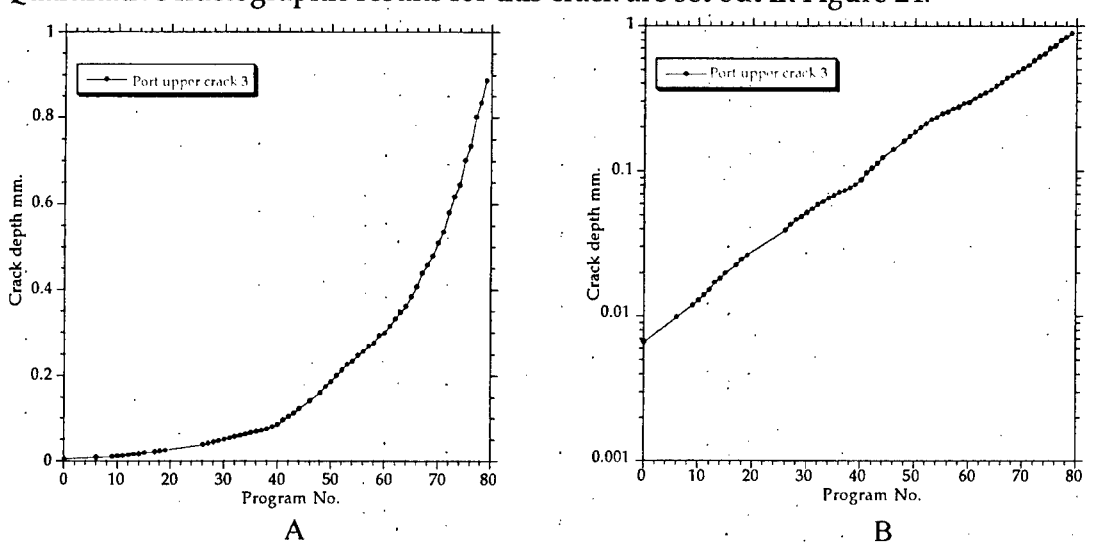

A B

Figure 24. Two plots showing the results of quantitative fractography. Plot A – linear crack depth versus Program No. and B - crack depth on a Log scale versus linear Program No.

2.3.12 Port upper aft edge - Crack 4

This crack originated from multiple sites beneath the intact IVD coating on the aft face of the bulkhead. The crack grew forward into the bulkhead. The initiation sites were spread over about a 0.1mm length centred about 0.4mm from the hole edge. The numerous cracks joined to form a single crack front, Figure 25 view A. Small etch-pits, probably associated with grain boundaries, acted as the initiating flaws. Intersection with the wing-attachment hole probably occurred relatively late in the crack growth life - at a crack depth of about 300μm.

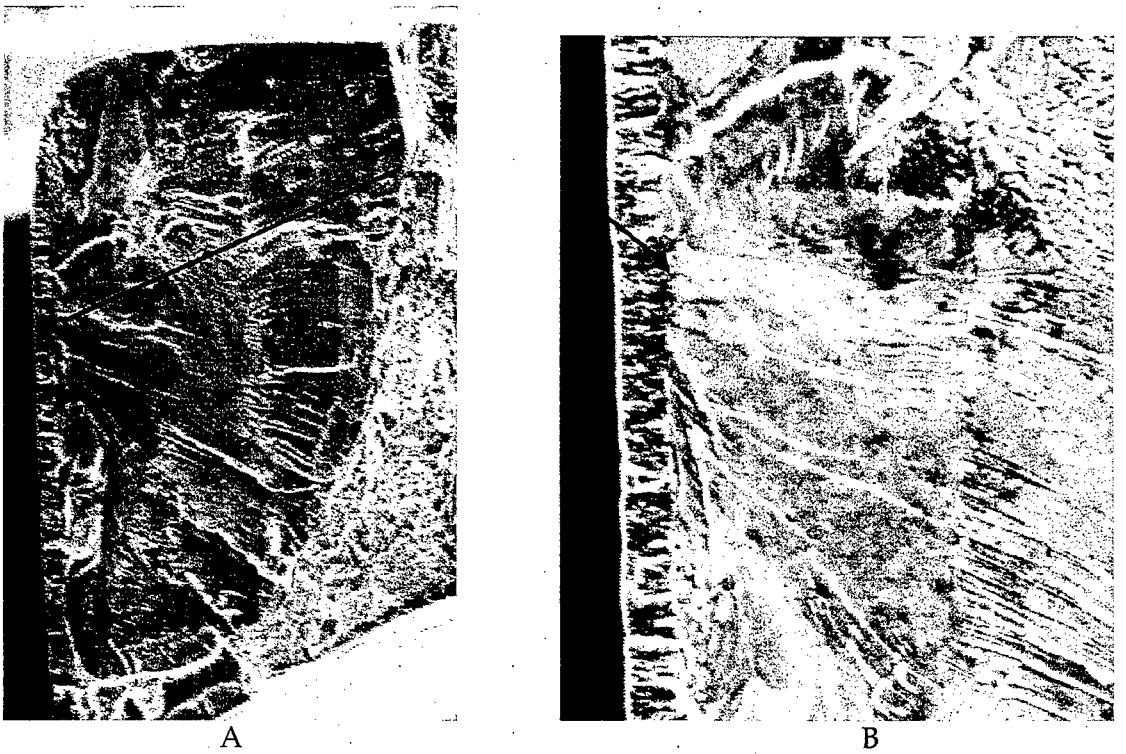

Figure 25. The crack profile and the initiation area for crack 4. The line shown in view A designates the approximate line followed during fractography. The cracking initiated beneath the IVD at the surface of the 7050.

Quantitative fractographic results for this crack are set out in Figure 26.

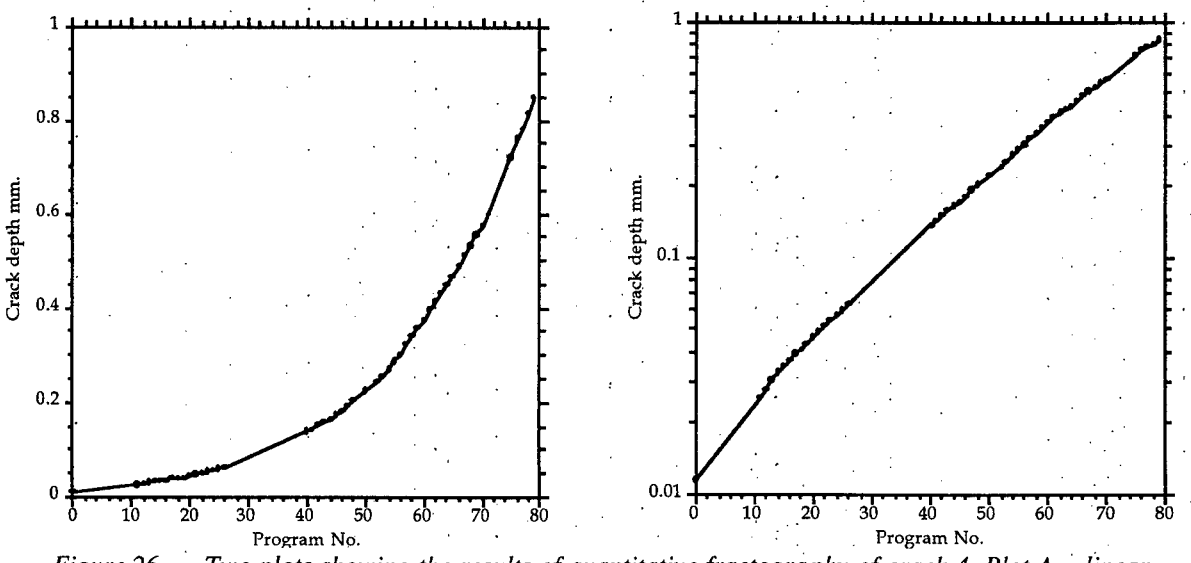

Figure 26. Two plots showing the results of quantitative fractography of crack 4. Plot A – linear crack depth versus Program No. and B - crack depth on a Log scale versus linear Program No.

2.3.13 Port upper aft edge - Crack 5

This crack originated from multiple sites beneath the intact IVD coating on the aft face of the bulkhead. A single main area of initiation was observed which had several closely spaced origins. These joined to form a single crack front, Figure 27A. Small etch-pits, probably associated with grain boundaries, acted as the initiating flaws. The crack grew with a 'thumbnail' shape, intersecting the hole relatively late in the crack's life - at a crack depth of about 150μm.

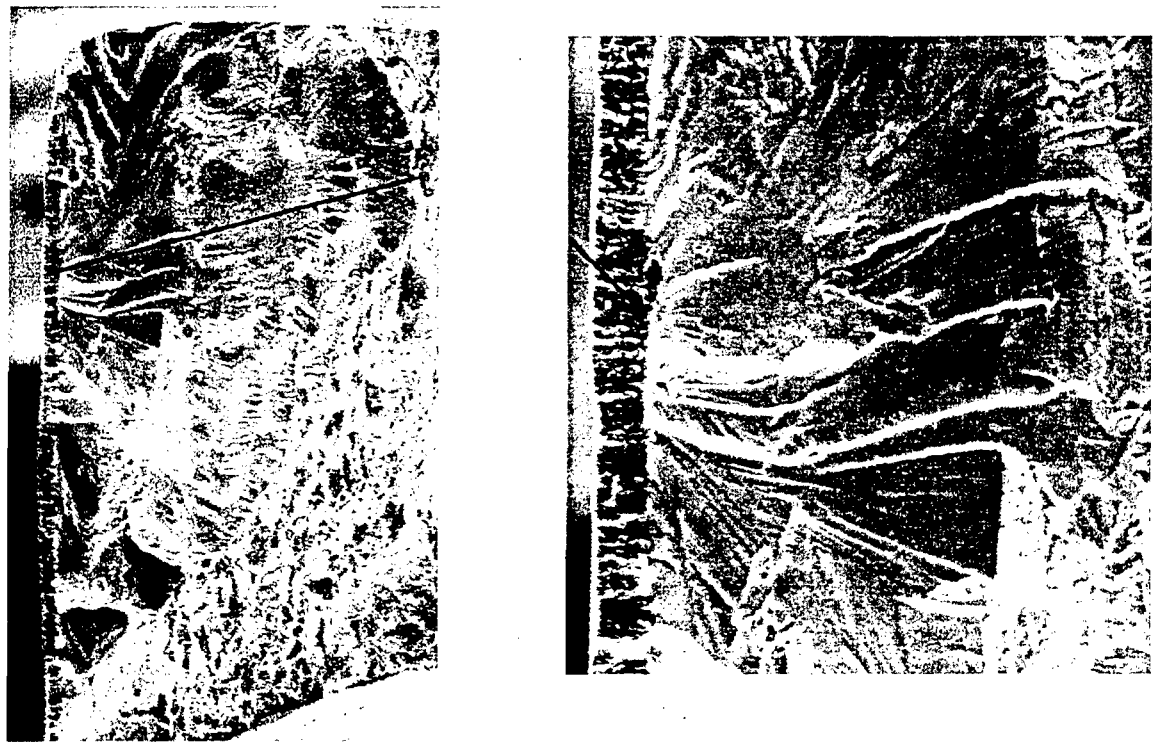

Figure 27. This Figure shows the crack profile and the initiation area for this crack. The line shown in view A designates the approximate line followed during fractography. The cracking initiated beneath the IVD at the surface of the 7050.

Quantitative fractographic results for this crack are set out in Figure 28.

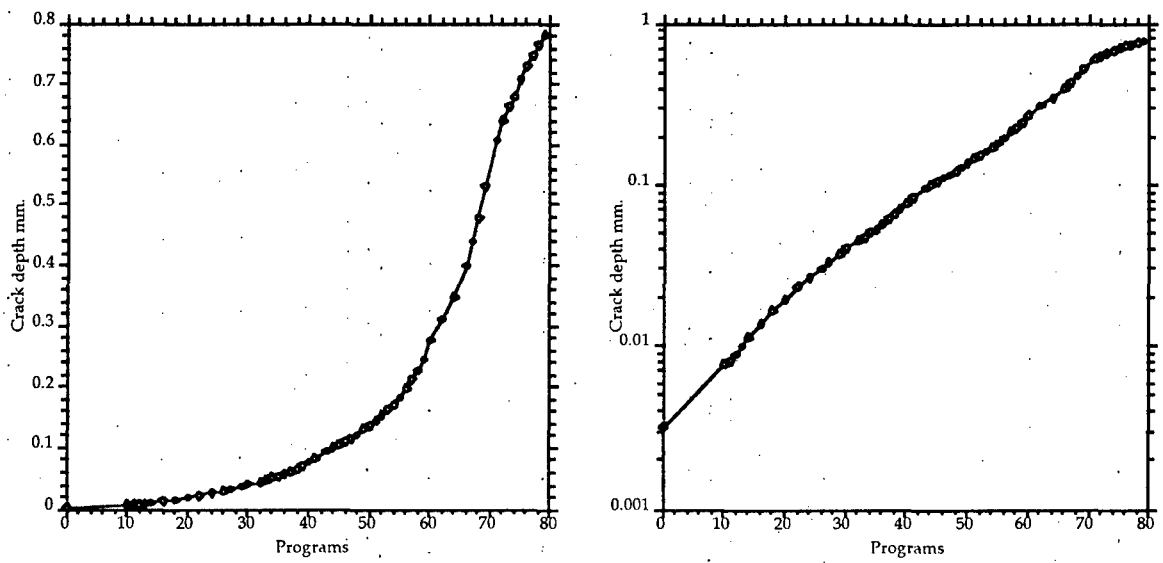

Figure 28. Two plots showing the results of quantitative fractography. Plot A – linear crack depth versus Program No. and B - crack depth on a Log scale versus linear Program No.

2.3.14 Port upper aft edge - Crack 6

This crack originated from multiple sites beneath the intact IVD coating on the aft face of the bulkhead. The crack grew forward into the bulkhead. A second crack was associated with the main crack. This second crack initiated from the same type of flaw, about 1mm from the hole edge. The initiation sites of the main crack were spread over about a 0.4mm length centred about 0.7mm from the hole edge. The numerous cracks joined to form a single crack front, Figure 29A. Small etch-pits, probably associated with grain boundaries, acted as the initiating flaws. Intersection with the wing-attachment-hole probably occurred late in the crack growth life - at a crack depth of about 450µm.

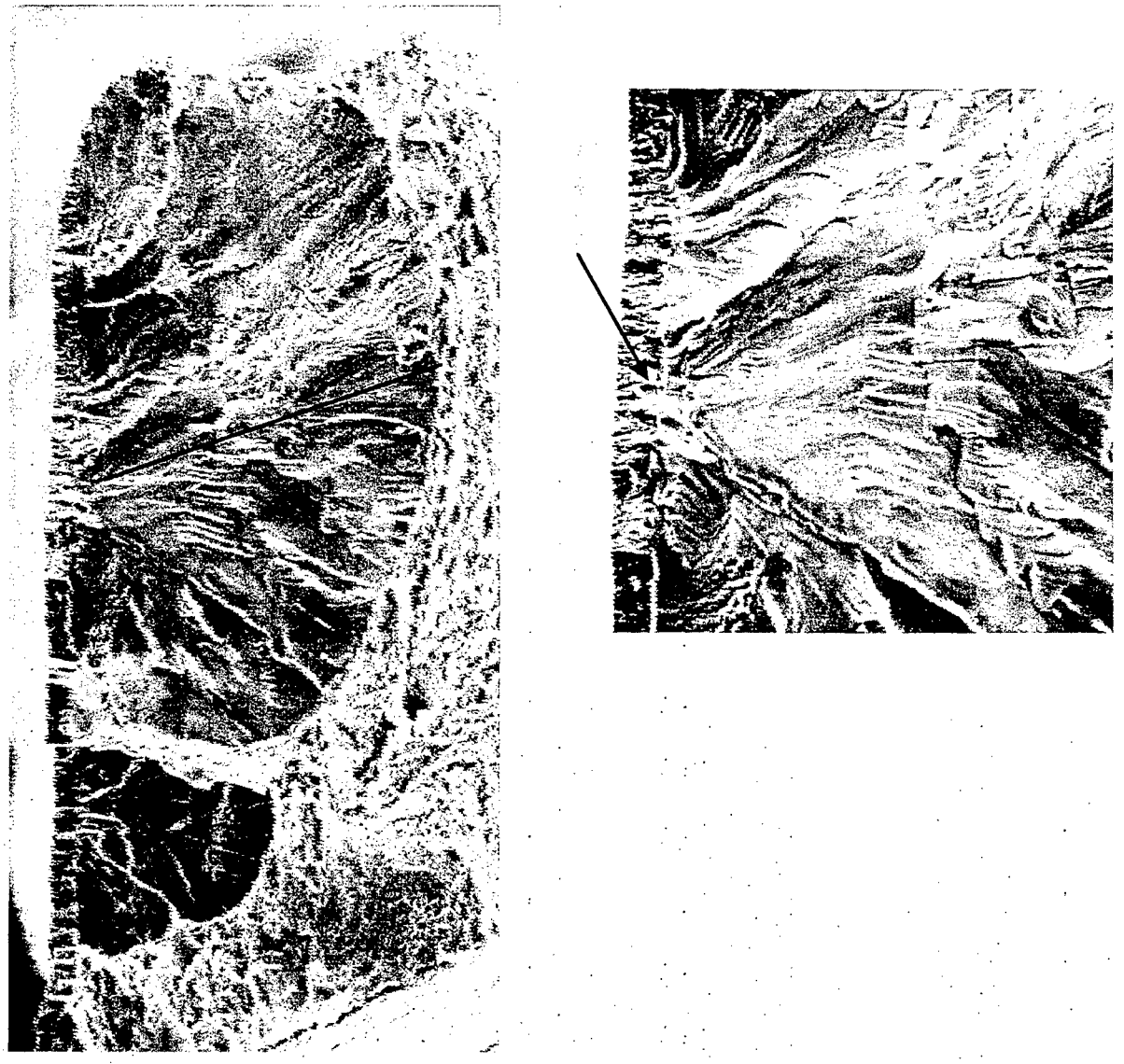

A B

Figure 29. A profile of crack 6 and its initiation area showing, 'A', a line that designates the approximate path followed during fractography. The cracking initiated beneath the IVD at the surface of the 7050.

Quantitative fractographic results for this crack are set out in Figure 30.

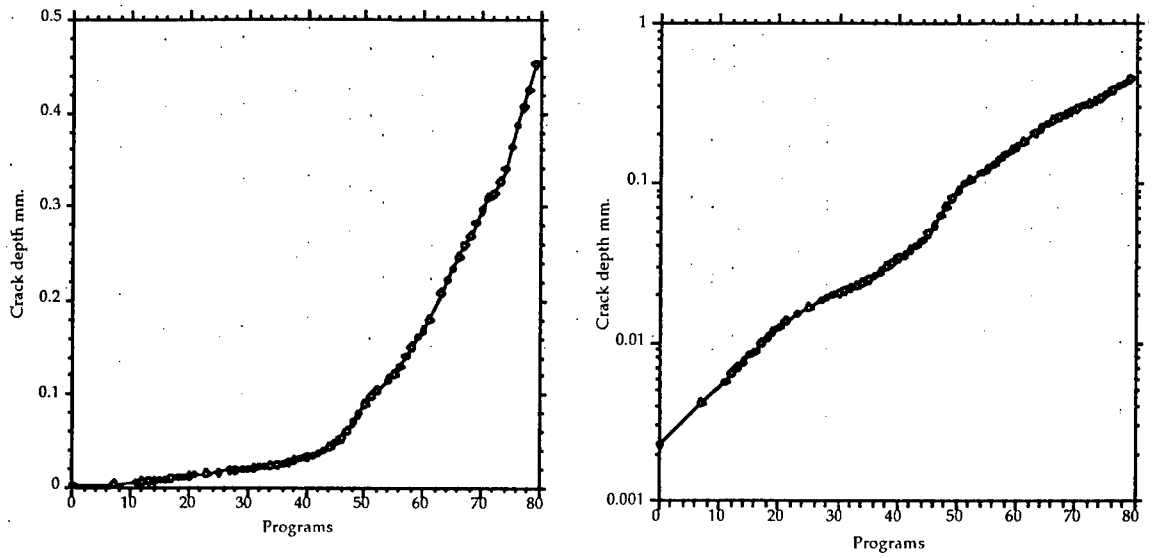

Figure 30. The quantitative fractography results. Plot A – linear crack depth versus Program No. and B - crack depth on a Log scale versus linear Program No.

2.3.15 Port upper aft edge - Crack 7

This crack originated from several sites beneath the intact IVD coating on the aft face of the bulkhead. The main crack grew forward into the bulkhead, linking with other cracks as it went. The initiation sites were typical of these cracks; they were associated with the etched grain boundaries at the 7050 surface beneath the IVD coating. These cracks joined to form a single crack front, Figure 31A, weighted towards the hole. Intersection with the hole probably occurred relatively late in the crack growth life - at a crack depth of about 300μm.

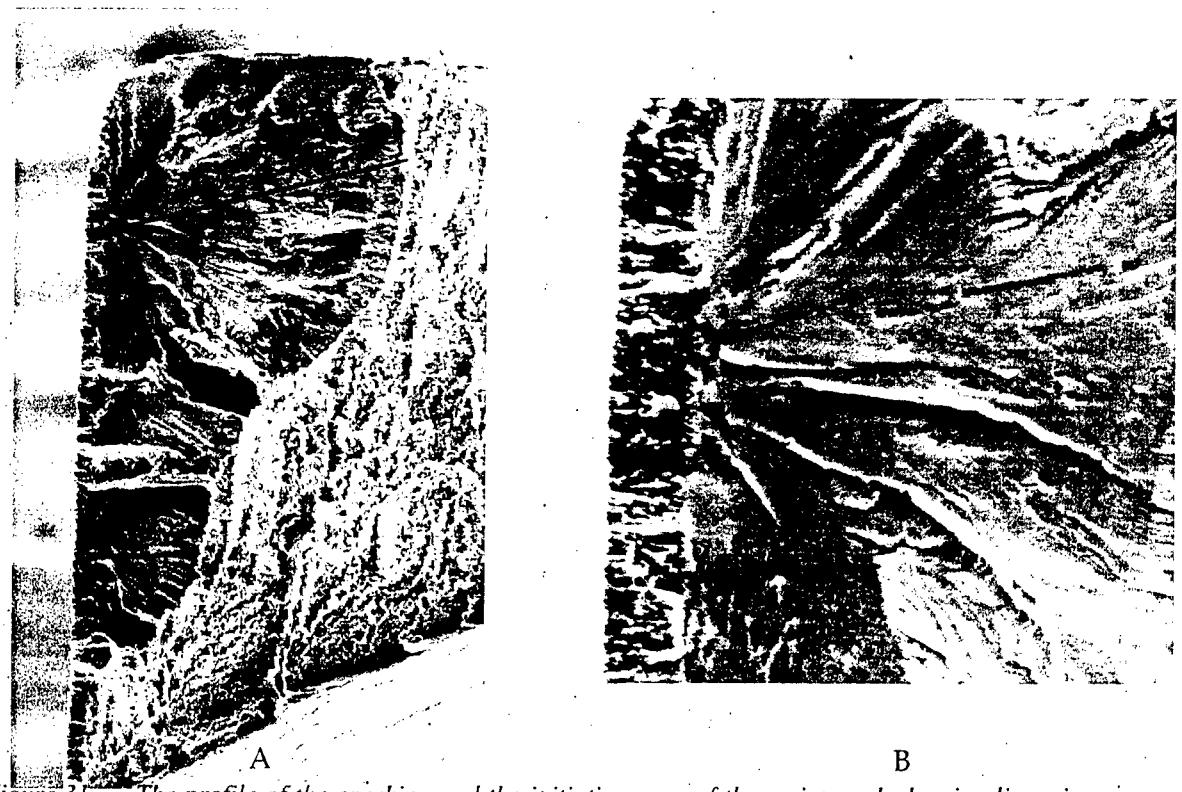

Figure 31. The profile of the cracking and the initiation area of the main crack showing lines, in view A, that designate the approximate paths followed during the fractography. The largest crack initiated beneath the IVD at the surface of the 7050, as did the other smaller cracks.

Quantitative fractographic examination was carried out on the main crack and one of the smaller cracks. The approximate tracks of these two crack growth plots are shown in Figure 31, and the results of the fractography in Figures 32 and 33.

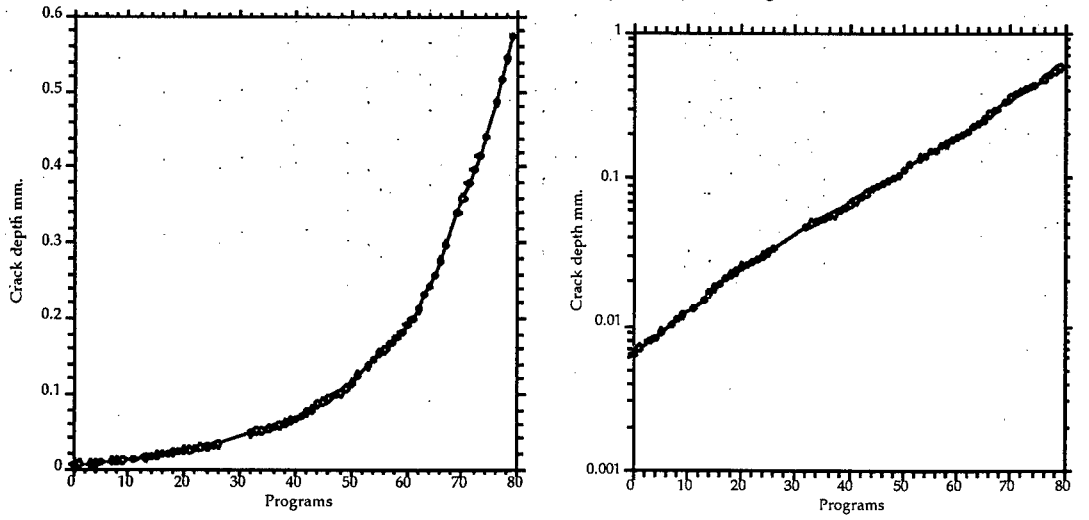

Figure 32. The quantitative fractography results. Plot A – linear crack depth versus Program No. and B - crack depth on a Log scale versus linear Program No.

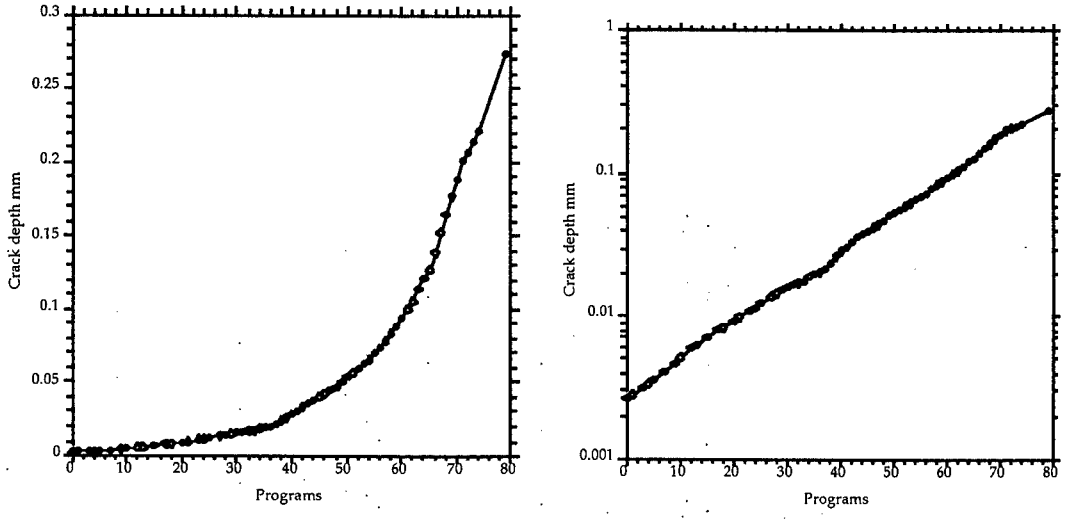

Figure 33. The quantitative fractography results. Plot A – linear crack depth versus Program No. and B - crack depth on a Log scale versus linear Program No.

2.4 Metallography

Several sections were cut from the pieces removed from the edges of the wing-attachment holes. These cuts were adjacent to the cracking. Examples of two of the sections are shown in Figure 34 A & B. These views were cut at right angles (A is looking at the plate edge and B is looking at the plate end). The general microstructure revealed was fine grained (average grain size about 10μm) with larger, elongated grains (50 to 100 μm). On a larger scale the fine grain material tends to form islands surrounded by the coarse grained material. Many large inclusions were visible although they were mostly elongated or broken up, rather than 'Y' shaped (from solidification) as has been observed with 7050 plate of poorer quality [2]. The structure revealed was produced during re-crystallisation, which can, apart form other sites in the material, initiate at inclusions. As the largest inclusions are usually associated with the largest grains it is probable that these inclusions initiated grain growth during re-crystallisation either faster or earlier than the other initiation sites, leading to excessive grain growth for those grains associated with the large

inclusions. This is consistent with the inner part of the plate having more large grains, due to the longer time that this region has to cool from the re-crystallisation temperature

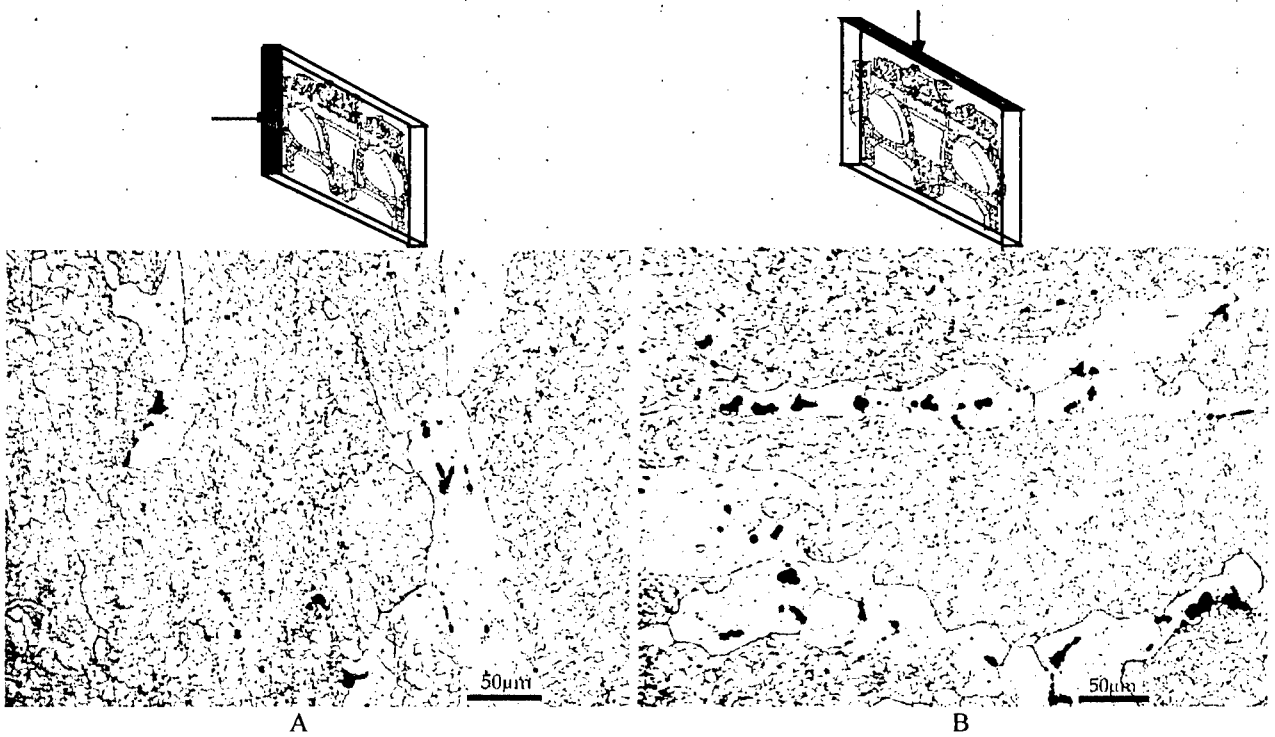

Figure 34 *The general microstructure of two sections through the port upper aft sliver. Note that these sections show the duplex grain size and the massive inclusions associated with the large grains.*

The section through the piece removed from the edge of the port upper aft hole revealed the extent of the step caused by the copper alloy bush in the hole - Figure 35. Examining the material beneath where the bush had resided revealed that deformation of the grain structure could be seen at the step but not beneath the bush its self (Figure 36).

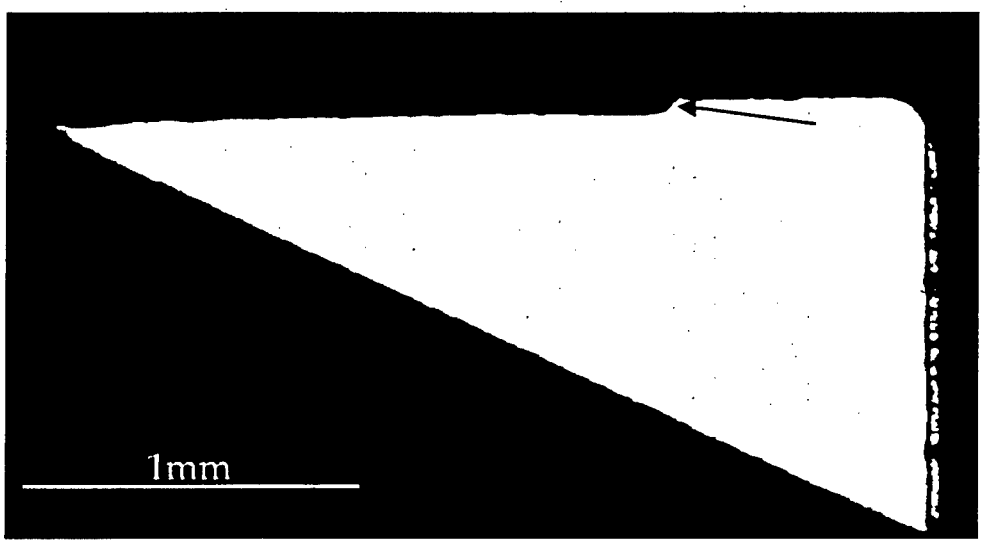

Figure 35 *Section through the piece removed from the edge of the port upper aft hole revealed the extent of the step (arrow) caused by the copper alloy bush in the hole.*

Figure 36 *Close view of the piece shown in Figure 35 showing the 7050 aluminium alloy etched. Distortion of the grains at the step can be seen, while no distortion of the grains can be seen in the area that was under the bush.*

Sections through the aft surface of the bulkhead taken from the removed pieces of material revealed etching defects. These were the type responsible for the initiation of fatigue cracking in the starboard and port upper aft edges of the wing-attachment holes. A number of examples of these defects along with cracks that, in some cases grew from them, are shown in Figures 37, 38 & 39.

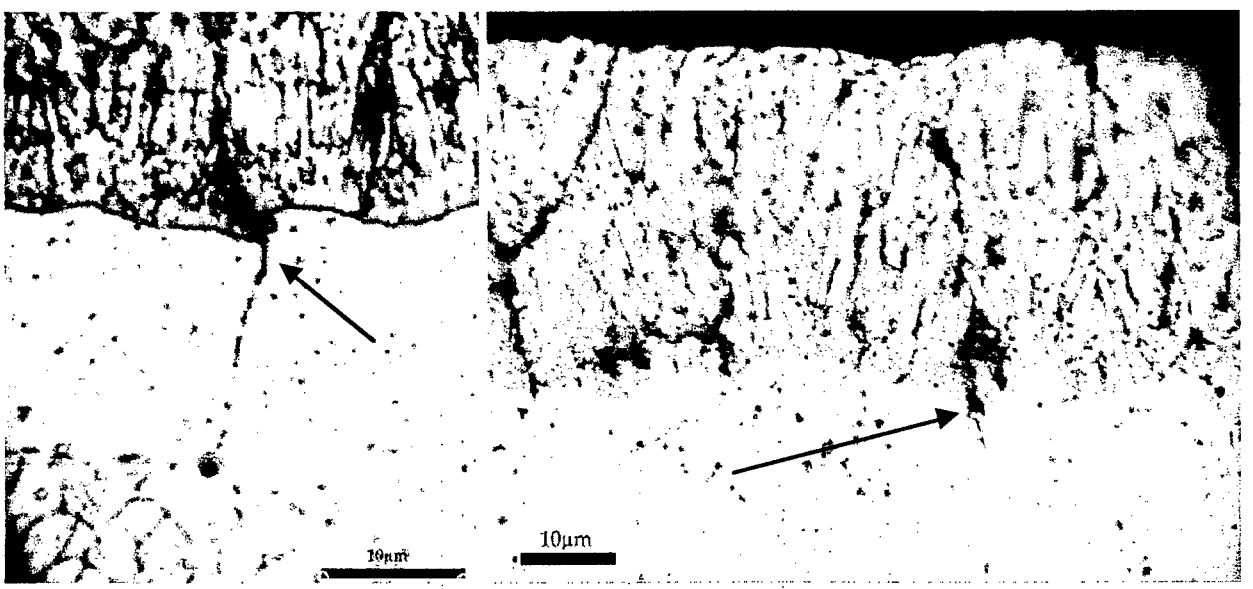

A B

Figure 37 *Penetrations produced at the grain boundaries (arrows) of the 7050, beneath the IVD layer can be seen in both these sections. The IVD appears as a porous columnar layer over the 7050. Note view A is etched with Keller's Reagent, View B is unetched.*

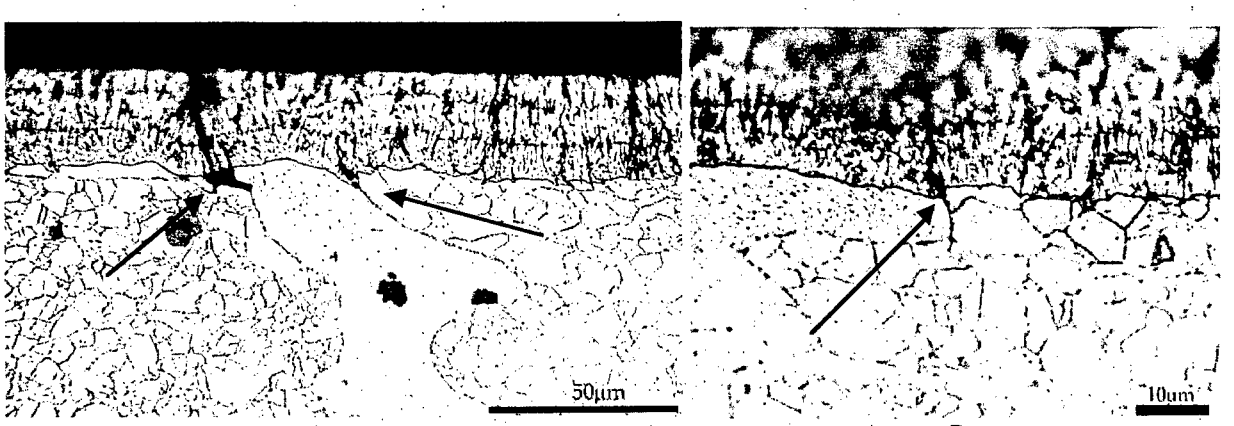

A B

Figure 38 *More examples of penetrations produced at the grain boundaries (arrows) of the 7050, beneath the IVD layer. Note both views are etched with Keller's Reagent.*

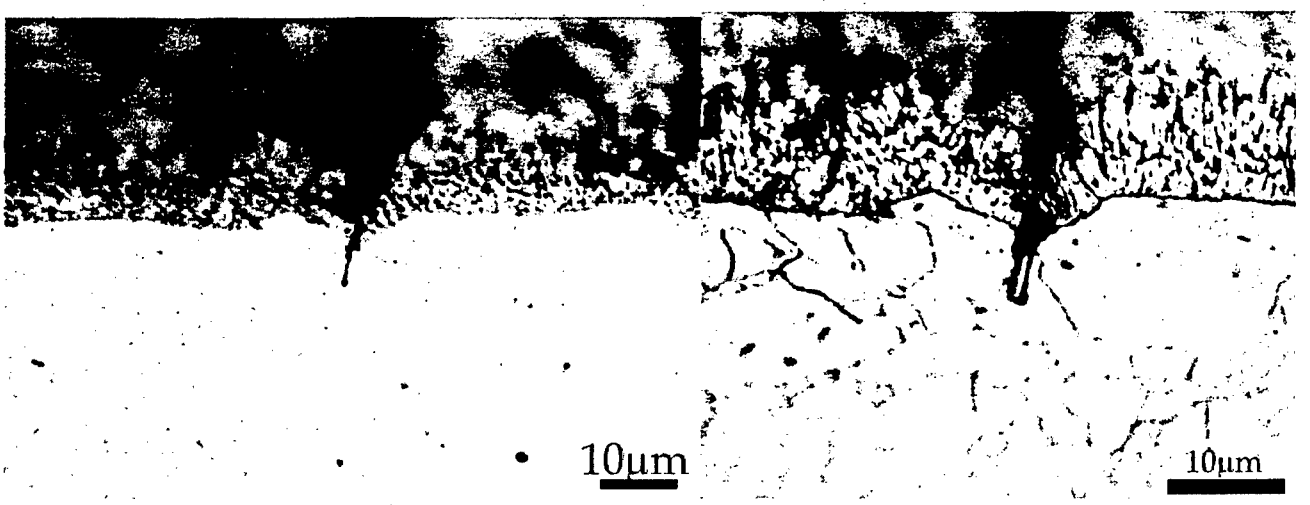

Figure 39. *Two views of the same defect in the unetched and etched condition showing a small crack-like defect, clearly growing from a surface etch pit, beneath the IVD coating. This etch pit was also clearly associated with a grain boundary. Note view B is etched with Keller's Reagent.*

During the examination of these sections several smaller fatigue cracks were disclosed. An example of one of these cracks is shown in Figure 40

Figur 40. *One of the smaller fatigue cracks found during sectioning of a piece (between crack 3 and 4) of the port upper aft wing-attachment hole edge. The crack is gaping due to loading during the breaking open of other cracks. Note that where the crack grows through the large grain the crack path is very straight.*

Although a number of very small cracks were revealed during this part of the examination it became clear that these crack were probably either growing very slowly or had arrested. In one case it appeared that a crack had arrested when it meet an inclusion while still very small - Figure 41 - suggesting that the applied stressing was insuficient at this crack size to progress the crack through the inclusion.

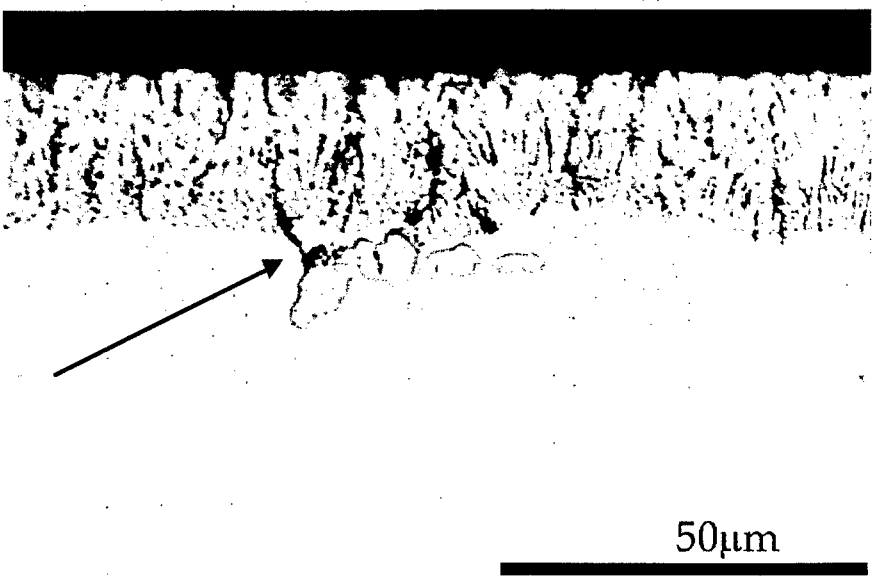

Figur 40. *One of the very small fatigue cracks found during sectioning of a piece (between crack 3 and 4) of the port upper aft wing-attachment hole edge. The crack (arrow) appears to have arrested when it meet an inclusion. Note also that there appears to be a crack in one of the inclusion that has not propagated a fatigue crack. (second inclusion from the left)*

3. Discussion

3.1 Summary of results

3.1.1 Upper wing-attachment holes

In all cases the cracking from both of the upper wing-attachment holes initiated on the aft face beneath the IVD layer - no cracks were seen to initiate at the corner of the hole. The initiating flaws (those that had not been removed) were consistent – etch grooves or pits - produced by the etching process used to clean the bulkhead prior to the IVD coating being applied. These grooves were the result of preferential attack of the 7050 grain boundaries.

In all cases, cracking had not extended beyond 1mm (forward) into the bulkhead.

Quantitative fractography of several cracks from each of these two holes were carried out. Summaries of the crack growth curves produced are presented in Figure 41 and 42. The crack growth data was plotted using log/linear axes in Figure 42, as this procedure has been found to reduce the data towards a straight line. This procedure was based on observations of a large number of program loaded fatigue tests [4] as well as data from service fatigue cracking, previous 488 bulkhead tests and numerous 7050 six inch radius fatigue tests using several different spectra [4, 5, & 6]. All of the curves produced in this analysis were found to show reasonably consistent results. The crack growth in most cases did approximate a straight line between depths of about 10μm to 1mm when plotted on a log/linear scale. (Such straight-line behaviour is similar to the constant-amplitude loading case where crack growth is a function of $(\Delta K)^2$) [5 & 6].

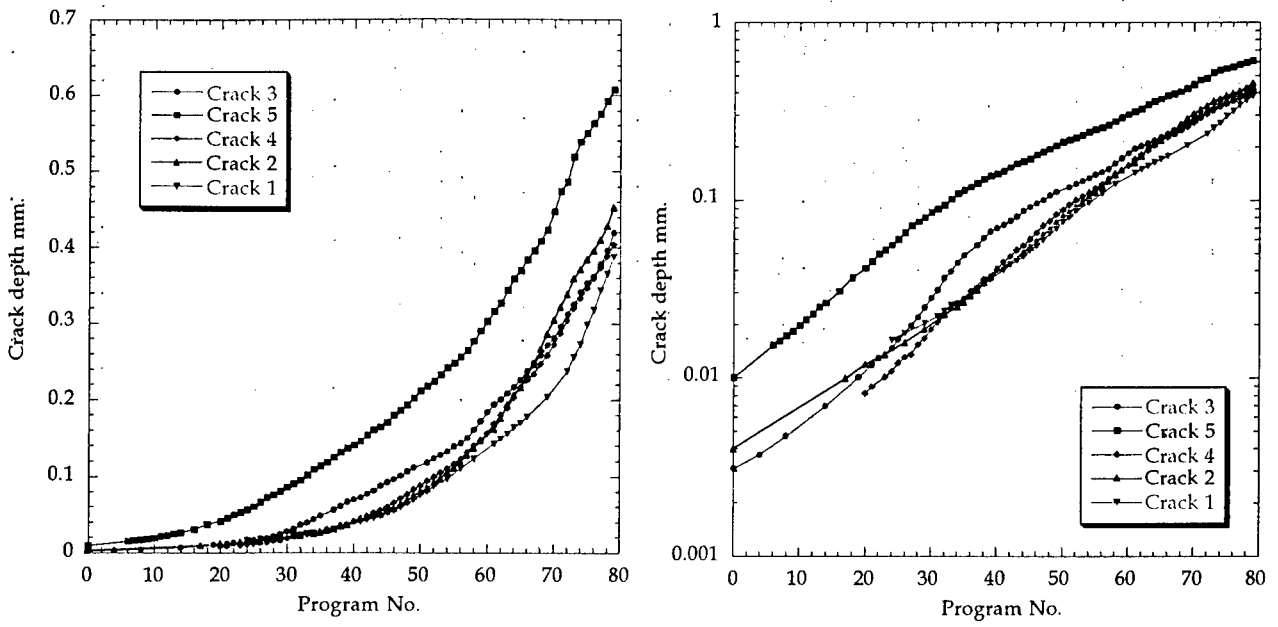

Figure 41 A plot of the growth of the cracks from the starboard upper wing-attachment hole

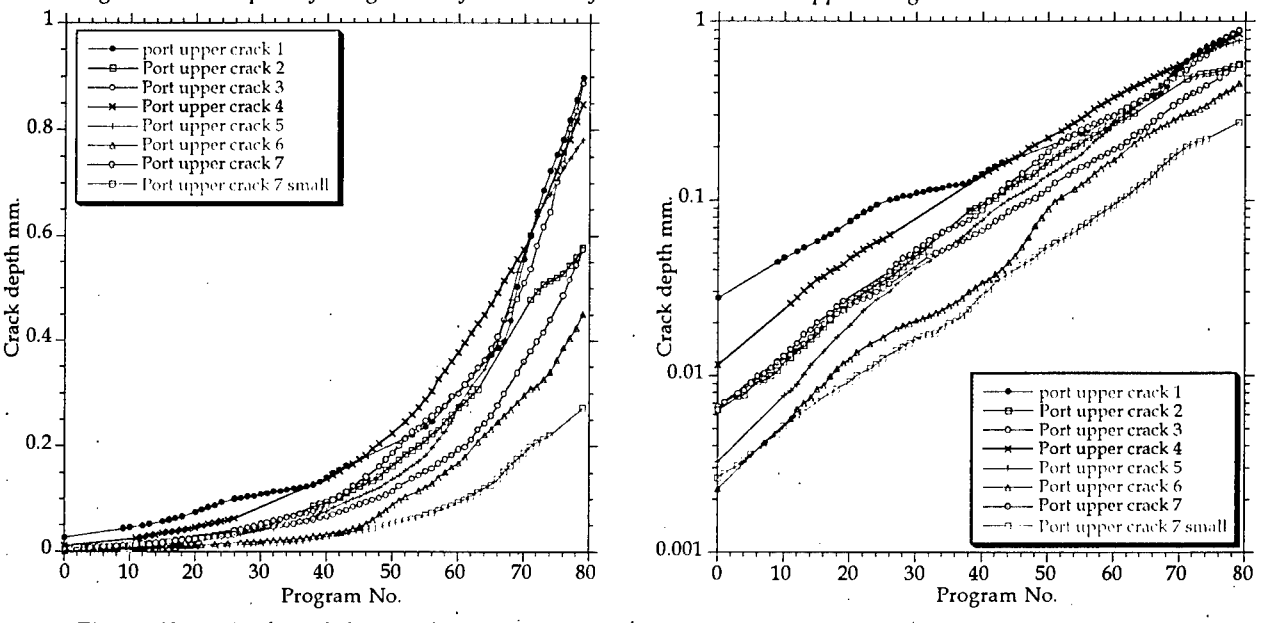

Figure 42 A plot of the crack growths from those cracks examined from the port upper wing-attachment hole

The crack positions in both the upper holes indicated that the microstructural orientation of grains intersecting the aft face of the bulkhead had little effect on the position of cracks. In both cases the cracking was found to be over about 90° of the circumference of the hole ie. the crack plane changed considerably for the cracks at either end of the slivers. Noting that the IVD coating was fairly consistently distributed around the entire circumference of all the wing-attachment holes, on both sides of the bulkhead, there is an implication that the areas around the holes, where this cracking was found must be the most highly stressed. Given also that the initiating defects were not cracked inclusions (in fact cracks in inclusions did not appear to lead to propagating fatigue cracks by this stage of testing) then two conclusions can be reached:

1. The stresses were insufficient to propagate fatigue cracks from cracked inclusions, or indeed to crack inclusions (the cracked inclusions observed were probably the result of surface deformation during bulkhead manufacture rather than cracking of the inclusions during the fatigue test).

2. The peak stresses were close to the lower limit for effective fatigue initiation given the type and range of initial flaws available, remembering that this fatigue test has now received greater than $3x10^8$ cycles.

3.1.2 Lower wing-attachment hole

In all cases, the starboard lower wing-attachment hole cracking was found to have initiated from mechanical damage at the edge of the hole. No cracks appeared to have initiated from beneath the IVD as had occurred with the upper holes. The two crack growth curves, plotted on the same axis, are presented in Figure 43. Crack one is consistent with upper-hole cracks in form and the growth nature; the main difference is that this crack appears to have initiated from a large flaw in comparison with the upper-hole cracks. This would be consistent with the initiation occurring from the lip. The lip may have, split to form an initial crack (possibly during formation), or it may have had high residual tensile stress that produced very rapid initial crack growth. The examination of the fracture through the lip region suggested the latter. Relatively high-K type fatigue growth markings could be seen in this region.

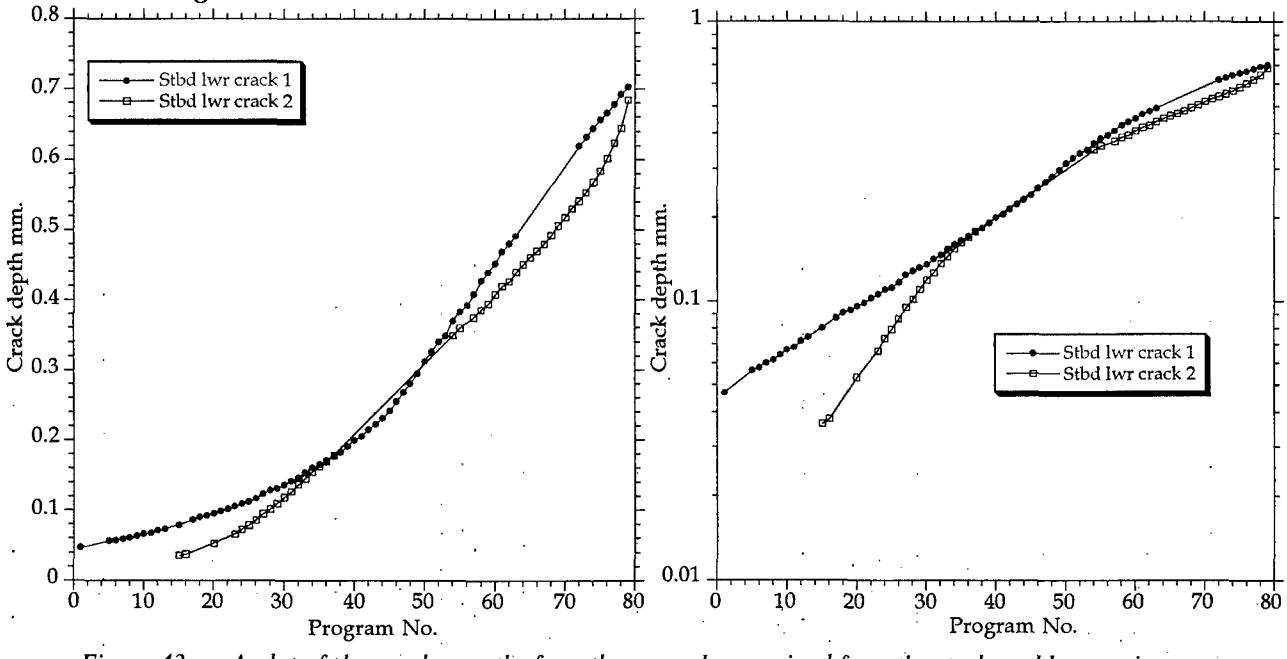

Figure 43 A plot of the crack growths from those cracks examined from the starboard lower wing-attachment hole

The second crack grew much faster than the first crack up until about 150µm. This was probably the result of local tensile residual stresses having an effect to about this depth. Following this region the crack appears to grow at about the same rate as crack 1, probably controlled only by the inherent material crack resistance and the applied loading. This suggests that the severity of the mechanical damage and any associated residual stress was a greater aid to initiation and early fatigue growth (particularly of crack 2) than any other flaw in this area. Flaws in this area that did not initiate a significant crack may have included the etching of grain boundaries (as with the upper holes) and inclusions.

Clearly, the probability of initiation from etching flaws caused during the IVD process must be less than the probability of initiation from the mechanical damage found in the edge of the lower starboard hole. This would suggest that the stressing in this region is below a limit for the production of propagating fatigue cracks from flaws produced by the IVD process in this material.

3.2 Comparison of results from each hole

The fractography results were combined and are presented in Figures 44 and 45. Curve fitting each of the data sets using the formula

$$a = a_o e^{bN}$$

gave a measure of the severity of the stressing for each crack position. The severity is indicated by the slope of the curve or 'b', while 'a_o' indicates the projected 'effective initial crack' size, which may differ from the measured initial flaw size. If the crack growth has a significant amount of linear growth on the log/lin presentation, then the 'b' constant will be a good measure of the likely growth rate in that position, regardless of the type or size of the initiating flaw. In fact, 'b' may be a material constant for a particular spectrum - combining the growth resistance factors which apply to the material. Interestingly the microstructural orientation did not appear to have a significant effect on these results. This leads to the notion that in order to estimate the life of a bulkhead area, both the 'a_o' (initial flaw size) and 'b' (stressing) must be known. Unfortunately the growth data produced to support life estimation is typically a combination of the initial flaw size and the growth to failure, with the final part of this growth distorted by tearing events. This results in difficulties if laboratory specimens do not adequately match the service component; there are significant differences in the initial flaws expected in carefully prepared laboratory specimens, made from material that may be non representative of service components. For instance most of the upper hole fatigue cracks initiated from flaws created by a combination of the IVD etching treatment and the microstructure of the 7050 plate, whereas initiation in laboratory specimens are nearly always found to occur at inclusions or mechanical damage (machining marks). It is noteworthy that inclusions did not initiate the cracking in the upper holes, and that there was evidence that inclusions could arrest very short cracks in these regions, given the large number of cycles that the bulkhead has recieved. Clearly, these differences along with a requirement to produce failures, in laboratory specimens, within a reasonable time, could result in the stressing of laboratory tests being higher than that required to produce the same cracking in the full-scale bulkhead.

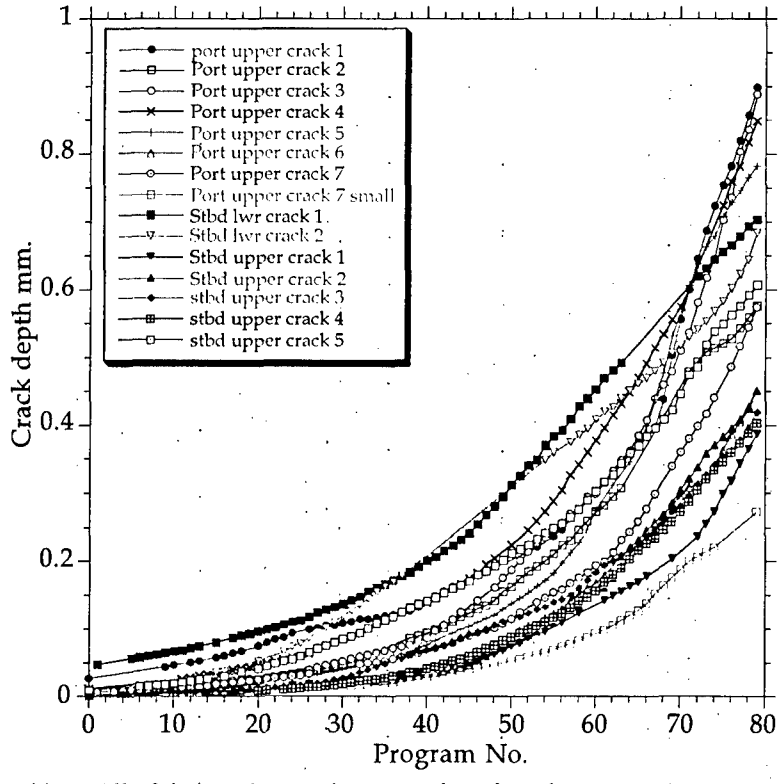

Figure 44. All of the crack growth curves plotted on the same axis.

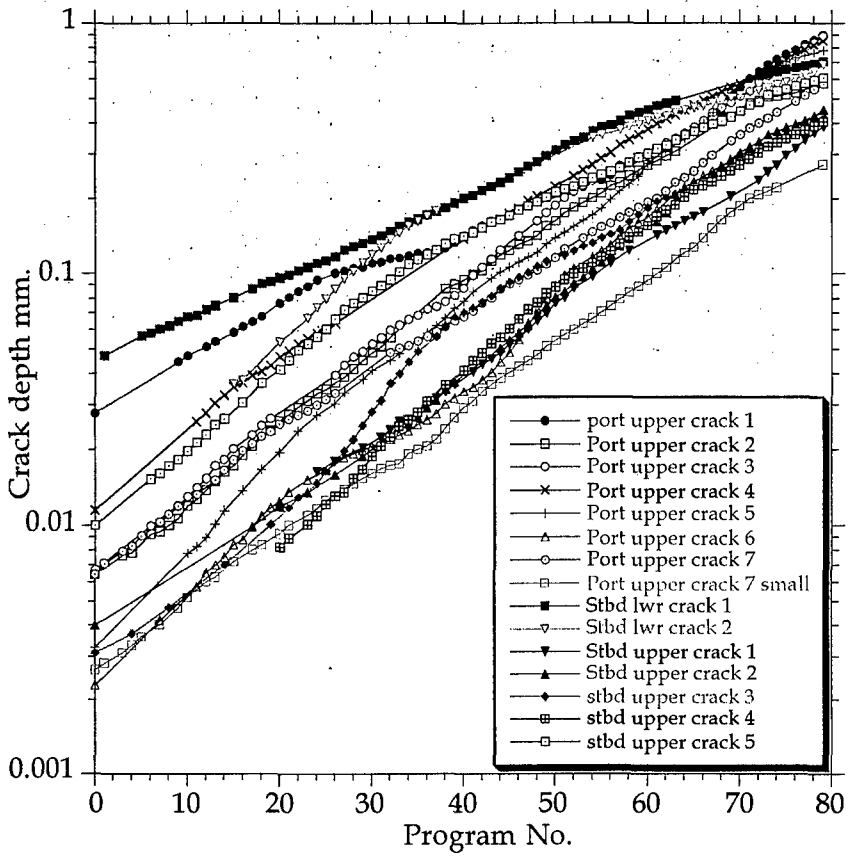

Figure 45. All of the crack growth curves plotted on the same axis- log/lin.

Table 2 presents the 'a_o' and 'b' results for each of the cracks. The second crack examined in the starboard lower hole had a growth curve that indicated that the early growth might have been influenced by a residual stress field (this field being caused by the associated damage). To produce a more accurate indication of the applied stressing in this area a second 'b' was calculated for the latter part of the cracking (the part that did not appear to have been affected by the residual stress).

Table 2

Crack position	a_o	b	b (corrected for main growth)	Estimated programs to 254μm	Estimated programs to 10mm	Crack depth (fractography) mm.
Stbd. Lwr. crack 1	0.047	0.036		47	149	0.70
Stbd. Lwr. crack 2	0.031	0.041	0.25	51	141	0.68
Stbd. upper crack 1	0.0038	0.058		72.	136	0.39
Stbd. upper crack 2	0.0031	0.064		69	126	0.45
Stbd. upper crack 3	0.0042	0.062		66	125	0.41
Stbd. upper crack 4	0.0026	0.067		68	123	0.40
Stbd. upper crack 5	0.016	0.050		55	129	0.61
Port upper crack 1	0.031	0.041		51	141	0.90
Port upper crack 2	0.0075	0.060		59	120	0.58
Port upper crack 3	0.0080	0.060		58	119	0.89
Port upper crack 4	0.016	0.052		53	121	0.85
Port upper crack 5	0.0048	0.067		59	114	0.78
Port upper crack 6	0.0049	0.066		60	115	0.45
Port upper crack 7	0.0075	0.055		64	131	0.57
Port upper crack 7 small	0.0027	0.059		77	139	0.27

Along with the 'a' and 'b' values, estimates of the number of programs to 'engineering initiation' (254μm or 0.01 inch) and to an approximate failure size (about 10mm, but probably greater) have been included. From these figures, it can be seen that even the fastest growing (highest 'b') crack would have probably lasted about 35 more programs (ignoring tearing effects at greater crack depths). Using the largest flaw with the fastest cracks, (a crack-like flaw of 50μm occurring in the starboard upper crack 5 or the port upper crack 5 positions) would have produced a 10mm crack in the 79 programs. These estimates assume that there is no influence from the residual stress produced by the cold expanded bushes in the holes. In reality the cracks would probably been retarded by these residual stresses with the result that even larger initial flaws could have been tolerated.

4. Conclusions

The investigation of the wing-attachment hole cracking revealed some interesting aspects of fatigue in this material, and its interaction with flaws and the microstructure;

1. Cracking was very consistent in both the upper holes, while the lower hole cracking appeared to have been influenced by either a large flaw, with a large 'effective crack size', or a significant residual stress.
2. Cracks from the upper holes all started from flaws created by the IVD coating process - none were found to have initiated from inclusions.
3. For this material and spectrum, the crack growth seemed to be relatively unaffected by the microstructure once a crack had reached a size greater than about 10μm.
4. The crack growth region can be depicted by a growth constant 'b' which allows extrapolation beyond the known data. This approach was also used to compare the severity of the different cracks, giving an indication of their expected life, and the effect of stressing, on the variation in crack growth rates from hole to hole.
5. The microstructure of the bulkhead in these regions was consistent with previously observed microstructure, although this material still had structures indicative of minimal breakdown from the original ingot. The re-crystallised grains appear to have had an influence on relief of the crack surface near the origins of cracks - large grain produced flat surfaces while smaller grains gave rougher surfaces.

5. References

1 S A Barter B Bishop & G Clark "Defect Assessment on F/A-18 488 Bulkhead Tested at ARL" Aircraft Material Report 125, AR-006-618, Department of Defence, Defence Science and Technology Organisation, Aeronautical Research Laboratory. August 1991.

2 S. A. Barter, N. Athiniotis & L. Lambrianidis "Examination of the Microstructure of Several Samples of 7050 Aluminium Alloy" Aircraft Materials Technical Memorandum, ARL-MAT-TM-403, AR-006-113, Department of Defence, Defence Science and Technology Organisation, Aeronautical Research Laboratories. August 1990.

3 P. K. Sharp, N. Athiniotis, R. Byrnes, S. A. Barter, J. Q. Clayton and G. Clark, "Assessment of RAAF F/A-18 FS488 Bulkhead Offcuts; Microstructure and Surface Condition" Technical Report DSTO-TR-0326, AR-009-679, Department of Defence, Defence Science and Technology Organisation, Aeronautical and Maritime Research Laboratory. 1996.

4. N. Athiniotis, S. A. Barter, T. Van Blaricum, G. Clark, and L. Sammut., "RAAF Macchi MB326H Centre Section Lower Boom Fatigue Testing" Technical Report DSTO-TR-0328, Department of Defence, Defence Science and Technology Organisation, Aeronautical and Maritime Research Laboratory. May 1996.

5. Goldsmith, N.T. and Clark, G., "Analysis and Interpretation of Aircraft Component Defects Using Quantitative Fractography", *in "Quantitative Methods in Fractography"* eds. Strauss, B.M. and Putatunda, S.K., STP 1085, publ. American Society for Testing and Materials, Philadelphia, USA (1990).

6. G. Clark, S. A. Barter and N. T. Goldsmith, "Influence of initial defect conditions on structural fatigue in RAAF aircraft", in "*Durability and Structural Reliability of Airframes*", (ed. A.Blom), EMAS, Warley.

DISTRIBUTION LIST

Fractographic Inspection of the Cracking FT488/2 removed at program 79

S A Barter

AUSTRALIA

Copy No.

DEFENCE ORGANISATION

Task Sponsor 1

S&T Program

Chief Defence Scientist
FAS Science Policy } shared copy
AS Science Corporate Management 2
Director General Science Policy Development 3
Counsellor Defence Science, London (Doc Data Sheet)
Counsellor Defence Science, Washington (Doc Data Sheet)
Director General Scientific Advisers and Trials/Scientific Adviser Policy and Command (shared copy) 4
Navy Scientific Adviser (Doc Data Sheet and distribution list only)
Scientific Adviser - Army (Doc Data Sheet and distribution list only)
Air Force Scientific Adviser 5
Director Trials 6

Aeronautical and Maritime Research Laboratory

Director 7
Chief of Airframes and Engines Division 8
Research Leader, Dr. C Martin 9
Head Fatigue and Fracture Detection and Assessment, Dr G Clark 10
S Barter:
D. Graham 11
M. Stimson 12
K. Sharp 13
CF TLO IFOSTP - Major N. Barrett 14

DSTO Library

Library Fishermens Bend 15
Library Maribyrnong 16
Library Salisbury (2 copies) 17,18
Australian Archives 19
Library, MOD, Pyrmont (Doc Data sheet only)
Library, MOD, HMAS Stirling (Doc Data sheet only)

Capability Development Division

Director General Maritime Development (Doc Data Sheet only)
Director General Land Development (Doc Data Sheet only)
Director General C3I Development (Doc Data Sheet only)

Air Force

ASI1 (SQNLDR T Saunder)	20

Corporate Support Program (libraries)

OIC TRS, Defence Regional Library, Canberra	21
Officer in Charge, Document Exchange Centre (DEC), 1 copy	22
*US Defence Technical Information Center, 2 copies	23,24
*UK Defence Research Information Centre, 2 copies	25,26
*Canada Defence Scientific Information Service, 1 copy	27
*NZ Defence Information Centre, 1 copy	28

Canada

Director Technical Airworthiness 3-8	29
National Research Council, Institute for Aerospace Research - D. Simpson	30
Bombardier, Services Division, CF-18 IFOSTP MGR.	31

SPARES (6 copies)

Total number of copies: **37**

DEFENCE SCIENCE AND TECHNOLOGY ORGANISATION
DOCUMENT CONTROL DATA

1. PRIVACY MARKING/CAVEAT (OF DOCUMENT)

2. TITLE
Fractographic Inspection of the Cracking FT488/2 Removed at Program 79

3. SECURITY CLASSIFICATION (FOR UNCLASSIFIED REPORTS THAT ARE LIMITED RELEASE USE (L) NEXT TO DOCUMENT CLASSIFICATION)

Document	(U)
Title	(U)
Abstract	(U)

4. AUTHOR(S)

S Barter

5. CORPORATE AUTHOR

Aeronautical and Maritime Research Laboratory
PO Box 4331
Melbourne Vic 3001 Australia

6a. DSTO NUMBER	6b. AR NUMBER	6c. TYPE OF REPORT	7. DOCUMENT DATE
DSTO-TN-0170	AR-010-649	Technical Note	September 1998

8. FILE NUMBER	9. TASK NUMBER	10. TASK SPONSOR	11. NO. OF PAGES	12. NO. OF REFERENCES
M1/9/555	98/195	DGTA	38	6

13. DOWNGRADING/DELIMITING INSTRUCTIONS

-

14. RELEASE AUTHORITY

Chief, Airframes and Engines Division

15. SECONDARY RELEASE STATEMENT OF THIS DOCUMENT

APPROVED FOR PUBLIC RLEASE

OVERSEAS ENQUIRIES OUTSIDE STATED LIMITATIONS SHOULD BE REFERRED THROUGH DOCUMENT EXCHANGE CENTRE, DIS NETWORK OFFICE, DEPT OF DEFENCE, CAMPBELL PARK OFFICES, CANBERRA ACT 2600

16. DELIBERATE ANNOUNCEMENT

NO LIMITATIONS

17. CASUAL ANNOUNCEMENT Yes

18. DEFTEST DESCRIPTORS

Fatigue, 7050 aluminium Alloy, Component fatigue testing, F/A-18 fatigue testing, 488 bulkhead fatigue testing, Fractography, Crack growth.

19. ABSTRACT

During the inspection of the FT488/2 Bare Bulkhead Fatigue Test specimen after 79 blocks of applied loading, cracking was found in several wing-attachment hole aft edges. Each of the cracked regions of the holes was cut from the bulkhead, sixteen of the cracks were broken open and the exposed crack surfaces were analysed. This analysis revealed several interesting aspects of fatigue crack growth in this bulkhead. These included the nature of the most (in this case) significant initiating flaws, the type (compared to other thick 7050 plate material) and effect of the microstructure on the growth of these cracks, and the relative growth rates of these cracks including estimates of the number of programs to failure.